

# Miocene emplacement and rapid cooling of the Pohorje pluton at the Alpine-Pannonian-Dinaridic junction, Slovenia

LÁSZLÓ I. FODOR<sup>1,\*</sup>, AXEL GERDES<sup>2</sup>, ISTVÁN DUNKL<sup>3</sup>, BALÁZS KOROKNAI<sup>1</sup>, ZOLTÁN PÉCSKAY<sup>4</sup>,  
MIRKA TRAJANOVA<sup>5</sup>, PÉTER HORVÁTH<sup>6</sup>, MARKO VRABEC<sup>7</sup>, BOGOMIR JELEN<sup>5</sup>, KADOSA BALOGH<sup>4</sup> &  
WOLFGANG FRISCH<sup>8</sup>

*Key words:* Alps, Miocene, magmatism, geochronology, thermobarometry, exhumation

## ABSTRACT

New laser ablation-inductive coupled plasma-mass spectrometry U-Pb analyses on oscillatory-zoned zircon imply Early Miocene crystallization ( $18.64 \pm 0.11$  Ma) of the Pohorje pluton at the southeastern margin of the Eastern Alps (northern Slovenia). Inherited zircon cores indicate two crustal sources: a late Variscan magmatic population (~270–290 Ma), and an early Neoproterozoic one (850–900 Ma) with juvenile Hf isotope composition close to that of depleted mantle. Initial  $\epsilon_{\text{Hf}}$  of Miocene zircon points to an additional, more juvenile source component of the Miocene magma, which could be either a juvenile Phanerozoic crust or the Miocene mantle. The new U-Pb isotope age of the Pohorje pluton seriously questions its attribution to the Oligocene age ‘Periadriatic’ intrusions. The new data imply a temporal coincidence with 19–15 Ma magmatism in the Pannonian Basin system, more specifically in the Styrian Basin. K-Ar mineral- and whole rock ages from the pluton itself and cogenetic shallow intrusive dacitic rocks (~18–16 Ma), as well as zircon fission track data (17.7–15.6 Ma), gave late Early to early

Middle Miocene ages, indicating rapid cooling of the pluton within about 3 Million years. Medium-grade Austroalpine metamorphics north and south of the pluton were reheated and subsequently cooled together. Outcrop- and micro scale structures record deformation of the Pohorje pluton and few related mafic and dacitic dykes under greenschist facies conditions. Part of the solid-state fabrics indicate E–W oriented stretching and vertical thinning, while steeply dipping foliation and NW–SE trending lineation are also present. The E–W oriented lineation is parallel to the direction of subsequent brittle extension, which resulted in normal faulting and tilting of the earlier ductile fabric at around the Early / Middle Miocene boundary; normal faulting was combined with strike-slip faulting. Renewed N–S compression may be related to late Miocene to Quaternary dextral faulting in the area. The documented syn-cooling extensional structures and part of the strike-slip faults can be interpreted as being related to lateral extrusion of the Eastern Alps and/or to back-arc rifting in the Pannonian Basin.

## Introduction

The Periadriatic Fault Zone (PFZ) represents a major, east-west trending Tertiary shear zone crosscutting the entire Alpine edifice from the Western Alps to the Pannonian Basin (inset of Fig 1a; Schmid et al. 1989). All along its strike the PFZ is associated with Paleogene intrusions (e.g. Laubscher 1983). Salomon (1897) was the first to apply the term “Periadriatic” for these plutons because of their intimate spatial relationship to the PFZ. Since most of these plutons exhibit Oligocene ages (28–34 Ma; for a thorough review see Rosenberg 2004), the term “Periadriatic” is also used, and will be used in this contribution, in a temporal sense (e.g. Laubscher 1983; Elias 1998; Rosenberg 2004).

The Karawanken tonalite (southern Austria, northern Slovenia; Fig. 1b) represents the easternmost outcrop of those Periadriatic intrusions. Its Oligocene age (28–32 Ma) is undisputed and well constrained by U-Pb (zircon), Rb-Sr (biotite), and Ar (amphibole, biotite) analyses (Scharbert 1975, Elias 1998). Further to the east, in the southwestern part of the Pannonian Basin, oil exploration wells reached tonalites below Tertiary sediments (Balogh et al. 1983; Körössy 1988). Radiometric ages (29–34 Ma) and detailed geochemical studies of these subsurface rocks clearly indicate that they also belong to the Periadriatic magmatic suite (Benedek 2002).

The Pohorje pluton (northern Slovenia), located 5–10 km north of the PFZ (Fig. 1a), was also regarded as part of the Periadriatic intrusions by many authors (Salomon 1897; Pamić &

<sup>1</sup>\*Geological Institute of Hungary, 1143 Budapest Stefánia 14, Hungary. E-mail: fodor@mafi.hu

<sup>2</sup>Institute of Geosciences, Altenhoferallee 1, 60438 Frankfurt am Main, Germany.

<sup>3</sup>Geoscience Center Göttingen, Sedimentology & Environmental Geology, Goldschmidtstrasse 3 D-37077 Göttingen, Germany.

<sup>4</sup>Institute of Nuclear Research, Hungarian Academy of Sciences, H-4026 Debrecen Bem tér 18/c, Hungary.

<sup>5</sup>Geološki Zavod Slovenije, Dimičeva 14, SI-1109 Ljubljana, Slovenia.

<sup>6</sup>Institute for Geochemical Research, Hungarian Academy of Sciences, H-1112 Budapest Budaörsi út 45, Hungary.

<sup>7</sup>University of Ljubljana, Department of Geology, Aškerčeva 12, SI-1000 Ljubljana, Slovenia.

<sup>8</sup>Institute of Geosciences, University of Tübingen, Sigwartstrasse 10, D-72076 Tübingen, Germany.

Pálinkáš 2000; Pálinkáš & Pamić 2001; Rosenberg 2004). Its distant location from the PFZ is not exceptional, since some other Periadriatic intrusions (e.g. Rieserferner pluton, Steenken et al. 2002) are also located along fault zones that are kinematically linked to the PFZ. However, Faninger (1970) concluded that Pohorje cannot be considered as an eastern prolongation of the Oligocene-age Karawanken pluton. Indeed, radiometric data do not support its assignment to the Periadriatic magmatic suite: Rb-Sr and K-Ar data yielded Miocene ages (19–16 Ma) for various rock types of the Pohorje pluton (Deleon 1969; Dolenc 1994). Recently, Fodor et al. (2002b) and Trajanova et al. (2008) presented K-Ar ages of different mineral separates and whole rock samples from the pluton, which all indicated Miocene ages. However, because of the possible thermal effects of the subsequent dacitic volcanism, hydrothermal-metasomatic alteration, and crystal-scale deformation, the interpretation of these data as emplacement ages was not entirely conclusive.

In this study we present new isotopic age data from the Pohorje pluton and spatially related dacites. The data set includes the results of U-Pb Laser Ablation-Inductive Coupled Plasma-Mass Spectrometry (LA-ICP-MS) dating of zircons, K-Ar dating on biotite, amphibole, feldspar and whole rock samples, and zircon fission track dating. These data clearly indicate a late Early Miocene age of the magmatic activity in the Pohorje Mountains. These new geochronological data, in combination with some structural observations, have implications for the structural evolution of the Alpine-Pannonian-Dinaric junction.

## Geological setting

The Pohorje (Bachern) and the Kozjak (Possruck) Mountains form the southeastern-most crystalline outcrops of the Eastern Alps and are located at the western margin of the Miocene Pannonian Basin system (Fig. 1a). They consist of basement and cover sequences of the Austroalpine nappe system formed during the Eoalpine orogeny (Frank 1987; Schmid et al. 2004). The deepest tectonic unit in the massif is mainly composed of medium-grade metamorphic rocks (gneiss, micaschist and amphibolite, intercalated with marble and quartzite, and sporadic eclogite lenses; Hinterlechner-Ravnik 1971, 1973; Mioč 1978). High-T retentivity isotopic data (Thöni 2002; Miller et al. 2005; Janák et al. 2007) from these rocks show that they underwent Eoalpine (ca. 90 Ma) high-pressure metamorphism. This rock pile is overlain by low-grade Palaeozoic and non-metamorphosed Permo-Triassic and Senonian sediments (Mioč & Žnidarčič 1977; Fig. 1a), which represent the uppermost tectonic unit in the study area. The original thrust contact between these units was reactivated and/or deformed during Late Cretaceous and Miocene exhumation phases (Fodor et al. 2002a).

The medium-grade metamorphic rocks were intruded by the Pohorje pluton, a 30 km long and 4–8 km wide magmatic body with ESE–WNW orientation (Fig. 1b). Although the boundary of the pluton is locally tectonized, the original magmatic contact, marked by a thin contact metamorphic aureole,

was mapped almost continuously along its margin (Mioč & Žnidarčič 1977; Žnidarčič & Mioč 1988). The Pohorje pluton was regarded either as a laccolith (Faninger 1970; Exner 1976), or alternatively, as a batholith (Trajanova et al. 2008).

Two larger occurrences of the host metamorphic rocks are located within the southeastern part of the pluton (Mioč & Žnidarčič 1977). The western one, near the peak of Veliki vrh (1344 m), is topographically and structurally located above the magmatic rocks and has a thermal contact aureole. The eastern one is a narrow, NW trending belt within the narrowing termination of the pluton (Fig. 1a).

The Pohorje pluton predominantly consists of tonalites and granodiorites (Dolar-Mantuani 1935; Faninger 1970; Zupančič 1994a; Altherr et al. 1995; Pamić & Pálinkáš 2000; Trajanova et al. 2008). Both intrusion and country rocks are cut by aplite, mafic and dacite dykes (Kieslinger 1935) and by small shallow subsurface dacite bodies.

Miocene sediments cover the older rock units in the north-western Pohorje Mountains. They continuously crop out in the Ribnica-Selnica trough, but appear only as scattered occurrences further north, on top of the Kozjak Mountains (Fig. 1). These sediments were tentatively correlated with more than 1 km thick marine successions of the Mura basin, where a late Early Miocene (Karpatic, 17.3–16.5 Ma) age was demonstrated (Márton et al. 2002; Jelen & Rifelj 2003, time scale according to Steininger et al. 1988). In the Ribnica-Selnica trough and on top of the southern Kozjak Mountains, the Karpatic sediments contain dacitic volcanoclastics and small intrusions (Fig. 1.; Winkler 1929; Mioč & Žnidarčič 1977).

## Results

### Geochronology

#### U-Pb and Hf isotope data

Zircons of sample 311 from the eastern part of the Pohorje pluton (Fig. 1b) were analysed for U-Pb and Hf isotopes by LA-ICP-MS at Frankfurt University, following the methods described by Gerdes & Zeh (2006, 2008). Spot-selection was guided by internal structures as seen in cathodoluminescence (CL) images of mounted and polished grains. Twenty-five U-Pb and 15 Hf isotope analyses were performed on core and mantle of 16 prismatic zircons (Fig. 2, Table 1a–b). Grains frequently display bright luminescent, rounded cores with relict oscillatory zoning. The oscillatory zoning is often blurred and widened, or fully replaced by CL-homogeneous domains. These cores are enclosed by variably wide CL-dark domains with well-developed oscillatory zoning typical of magmatic growth (zr1, 2, 4, 5, 8, 11 in Fig. 2a). Some CL-dark grains show no cores (zr6 in Fig. 2a), and in other cases the dark overgrowths form only ~20 µm wide rims around large cores (zr4–5 in Fig. 2a). Eleven spot measurements on the U-rich (1500–19800 ppm) CL-dark oscillatory-zoned domains yielded equivalent and concordant results with an age of  $18.64 \pm 0.11$  Ma ( $2\sigma$ ).  $^{206}\text{Pb}/^{238}\text{U}$  ages of

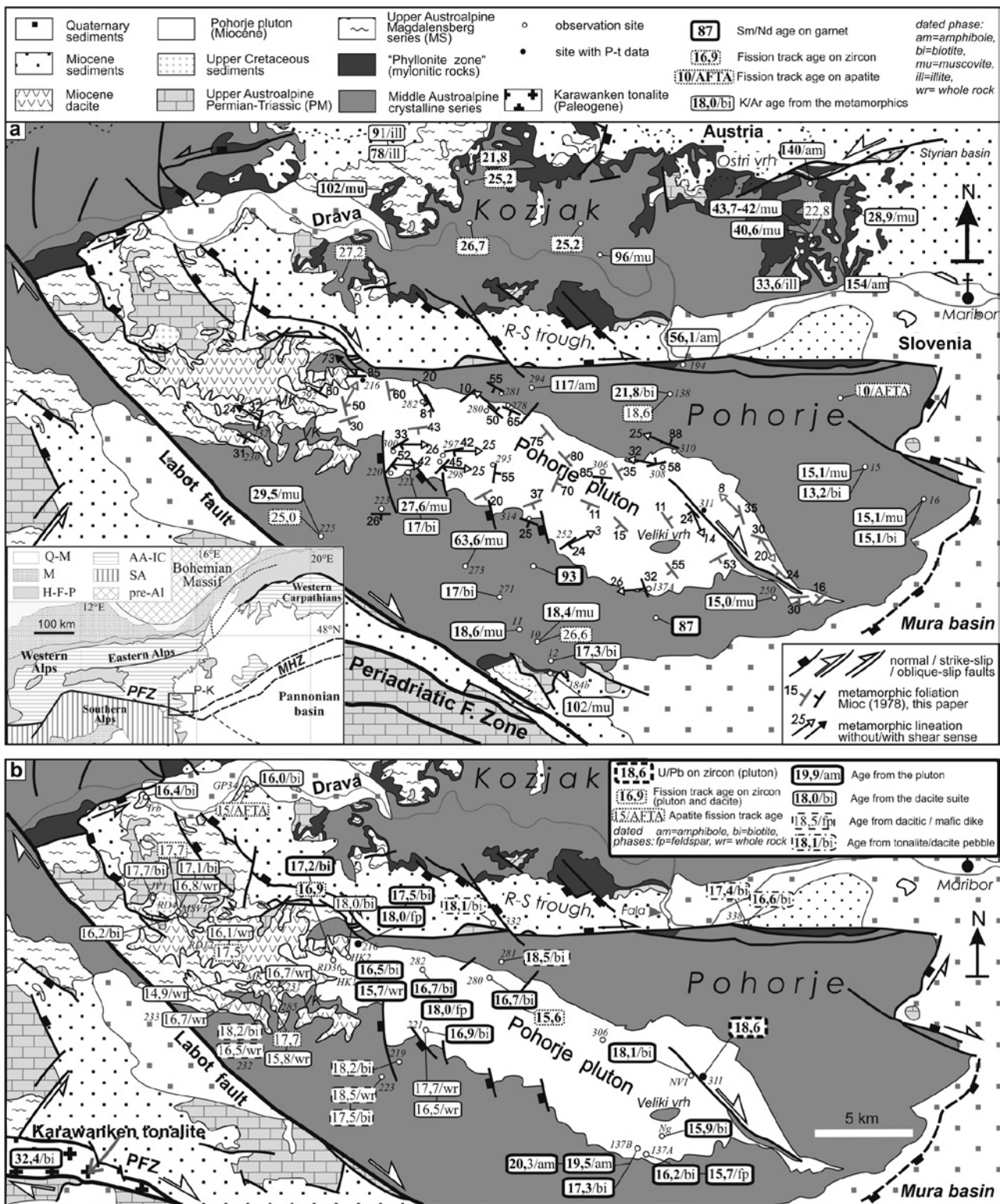


Fig. 1. Geological setting and geochronological data from the Pohorje Mountains 1a: Simplified geological map of the Pohorje Mountains with geochronological data of the metamorphic rocks. Foliation and lineation data of the Pohorje pluton (Mioč, 1978, Žnidarič & Mioč 1988, and our own measurements) are also shown. R-S trough: Ribnica-Selnica trough; VK: Velka Kopa. Insert shows tectonic sketch map of Eastern and Southern Alps and the western Pannonian Basin showing the location of the Pohorje and Kozjak Mountains MHZ: Mid-Hungarian Zone; Q-M: Quaternary-Miocene; M: Molasse; HFP: Helvetic, Flysch, Penninic units; AAIC: Austroalpine, Inner Carpathian units; SA: Southern Alps; pre-Al: pre-Alpine units. 1b: Geochronological data from the magmatic rocks. In cases of duplicate measurements from the same site (see Table 2), the average age is shown. MK: Mala Kopa.

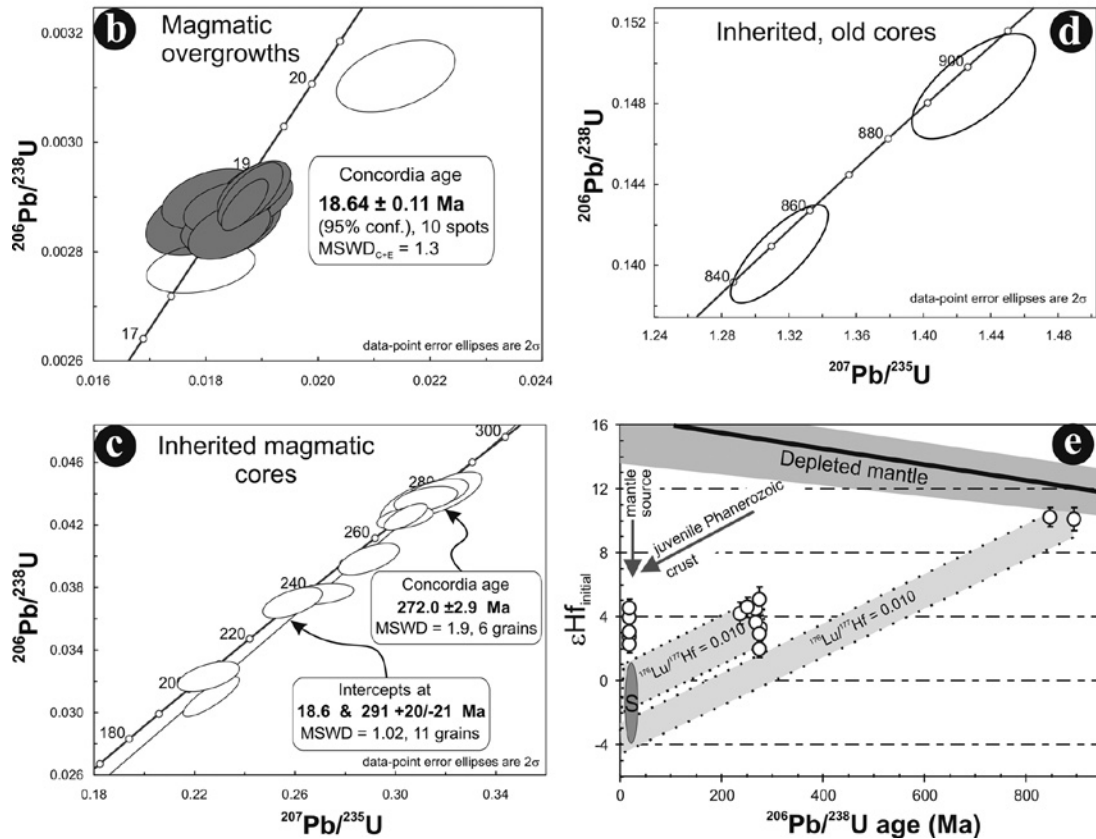
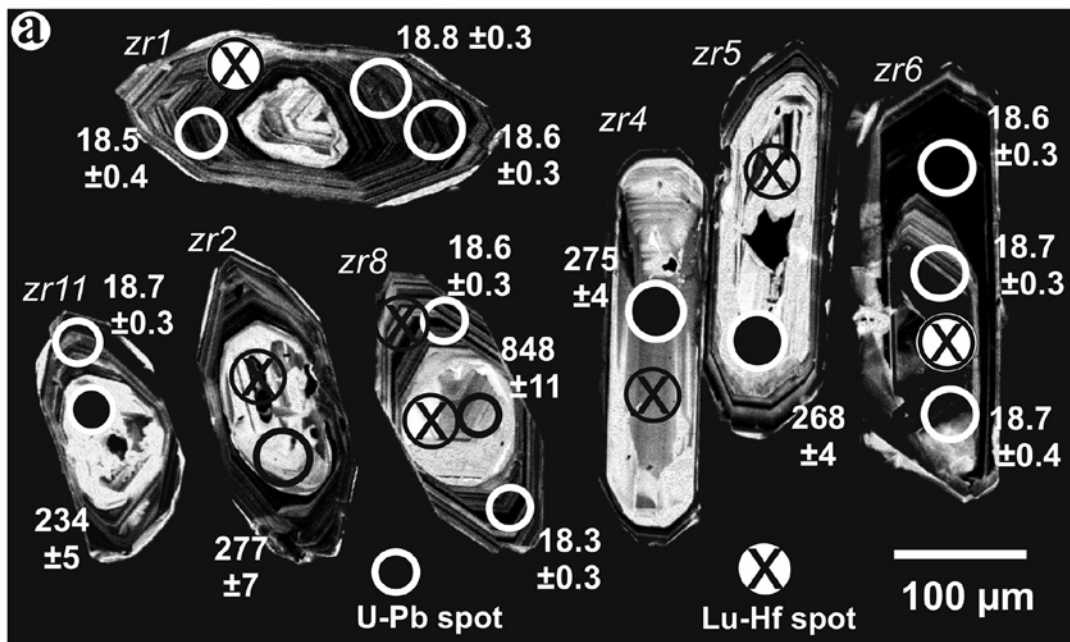


Fig. 2. U-Pb age and Hf isotope data from the eastern part of the Pohorje pluton (site 311). 2a: Representative cathodoluminescence images of zircon with location of U-Pb and Hf isotope spots and the corresponding U-Pb age with  $2\sigma$  error. Note the uniform age of oscillatory-zoned magmatic rims between 18.3–18.7 Ma. Inherited cores display two age populations of 270–290 Ma and 850 Ma, respectively. 2b, c, d: U-Pb concordia diagrams of the three distinct zircon age populations. 2e: Initial  $\epsilon\text{Hf}$  isotope composition versus  $^{206}\text{U}/^{238}\text{Pb}$  age of the different zircon domains. Grey field shows the evolution trend of the crust represented by the Permian and Neoproterozoic cores assuming a mean  $^{176}\text{Lu}/^{177}\text{Hf}$  of 0.010. Also shown is the composition of depleted mantle through time. Note that  $\epsilon\text{Hf}_{(t)}$  of Miocene zircon domains are more juvenile as the source component (field with dark S) inferred from the inherited cores. Grey arrows show two possible source components of the Miocene magma to explain the Hf isotope composition.

Table 1. U/Pb age data and Lu/Hf isotopic data from from the Pohorje pluton, sample 311.  
1a: Results of U/Pb LA-ICP-MS dating of zircons.

No.	$^{207}\text{Pb}^a$ (cps)	U <sup>b</sup> (ppm)	Pb <sup>b</sup> (ppm)	$\frac{\text{Th}^b}{\text{U}}$	$\frac{^{206}\text{Pb}^c}{^{204}\text{Pb}}$	$\frac{^{206}\text{Pb}^d}{^{238}\text{U}}$	$\pm 2\sigma$ (%)	$\frac{^{207}\text{Pb}^d}{^{235}\text{U}}$	$\pm 2\sigma$ (%)	$\frac{^{207}\text{Pb}^d}{^{206}\text{Pb}}$	$\pm 2\sigma$ (%)	rho <sup>e</sup>	$\frac{^{206}\text{Pb}}{^{238}\text{U}}$	$\pm 2\sigma$ (Ma)	$\frac{^{207}\text{Pb}}{^{235}\text{U}}$	$\pm 2\sigma$ (Ma)
zr1	1139	1621	4.3	0.09	1430	0.002872	2.0	0.01810	4.7	0.04571	4.3	0.42	18.5	0.4	18.2	0.9
zr1	4210	1539	4.2	0.09	8724	0.002887	1.4	0.01872	3.6	0.04703	3.4	0.38	18.6	0.3	18.8	0.7
zr1	5133	1859	5.1	0.10	10705	0.002921	1.6	0.01899	2.8	0.04715	2.4	0.56	18.8	0.3	19.1	0.5
zr2 c	4386	213	10	0.50	3104	0.04394	2.6	0.3193	3.9	0.05271	2.8	0.68	277	7	281	10
zr3 c	17030	83	15	0.96	24191	0.1489	1.4	1.4301	2.1	0.06967	1.5	0.68	895	12	902	13
zr4 c	2573	103	5.1	0.66	893	0.04360	1.5	0.3119	3.3	0.05188	2.9	0.46	275	4	276	8
zr5 c	12421	276	13	0.61	7641	0.04238	1.4	0.3036	3.0	0.05195	2.7	0.45	268	4	269	7
zr6	11027	6983	19	0.03	4442	0.002906	1.6	0.01820	3.9	0.04542	3.6	0.40	18.7	0.3	18.3	0.7
zr6	24384	19811	53	0.01	33199	0.002894	1.4	0.01882	1.8	0.04716	1.2	0.74	18.6	0.3	18.9	0.3
zr6	11317	7667	21	0.03	5256	0.002907	1.9	0.01884	3.1	0.04701	2.4	0.62	18.7	0.4	19.0	0.6
zr7	3315	2726	7.2	0.03	6814	0.002856	1.7	0.01860	3.8	0.04722	3.3	0.46	18.4	0.3	18.7	0.7
zr8	2499	1776	4.8	0.09	4288	0.002889	1.7	0.01852	3.7	0.04650	3.3	0.45	18.6	0.3	18.6	0.7
zr8	2834	2318	6.2	0.11	3963	0.002846	1.5	0.01853	3.2	0.04723	2.9	0.48	18.3	0.3	18.6	0.6
zr8 c	26231	321	48	0.43	38815	0.1406	1.4	1.3152	1.8	0.06786	1.1	0.79	848	11	852	10
zr9 c	9657	508	22	0.37	18462	0.04246	1.7	0.3038	2.3	0.05190	1.6	0.71	268	4	269	6
zr10 c	2932	263	11.6	0.40	5540	0.04391	1.9	0.3157	3.4	0.05214	2.9	0.54	277	5	279	8
zr11	2485	2012	5.4	0.04	5110	0.002900	1.5	0.01888	3.4	0.04721	3.1	0.44	18.7	0.3	19.0	0.6
zr11 c	10949	227	12	0.63	802	0.03692	2.2	0.2586	3.8	0.05079	3.1	0.59	234	5	234	8
zr12	1775	1418	3.7	0.07	3464	0.002776	1.4	0.01802	4.4	0.04706	4.2	0.32	17.9	0.3	18.1	0.8
zr12	11310	8488	23	0.02	5115	0.002910	1.7	0.01890	2.5	0.04711	1.9	0.67	18.7	0.3	19.0	0.5
zr13 c	2618	163	6.5	0.03	5344	0.04340	2.7	0.3095	4.1	0.05173	3.1	0.65	274	7	274	10
zr14 c	4699	168	8.2	0.95	622	0.03748	1.5	0.2697	4.1	0.05218	3.8	0.36	237	3	242	9
zr15 c	2675	82	3.6	0.47	3104	0.03973	2.1	0.2890	3.5	0.05275	2.8	0.60	251	5	258	8
zr16 c	13095	900	30	0.24	6961	0.03087	3.4	0.2259	4.1	0.05309	2.2	0.84	196	7	207	8
zr16	2327	1508	4.4	0.05	2099	0.003127	1.7	0.02149	4.0	0.04984	3.6	0.43	20.1	0.4	21.6	0.9
Plesov <sup>f</sup>	15255	628	32	0.11	20120	0.05392	1.3	0.3941	1.5	0.05307	0.7	0.72	338.5	4.8	337.4	4.1

c = zircon cores; <sup>a</sup> Within run background-corrected mean  $^{207}\text{Pb}$  signal in counts per second. <sup>b</sup> U and Pb content and Th/U ratio were calculated relative to GJ-1 reference and are accurate to about 10% due to heterogeneity of GJ-1. <sup>c</sup> measured ratio corrected for background and  $^{204}\text{Hg}$  interference (mean  $^{204}\text{Hg} = 198 \pm 22$  cps). <sup>d</sup> corrected for background, mass bias, laser induced U-Pb fractionation and common Pb (Gerdes and Zeh, 2006, 2008); Uncertainties are propagated by quadratic addition of within-run precision (2SE) and the reproducibility of GJ-1 (2SD; n = 12). <sup>e</sup> Rho is the error correlation defined as  $\text{err}_{206\text{Pb}/238\text{U}}/\text{err}_{207\text{Pb}/235\text{U}}$ . <sup>f</sup> mean (n = 12)  $\pm 2$  standard deviation of Plesovice reference zircon (cf. Slama et al. 2008).

1b: Lu/Hf isotopic data of zircons

No.	$^{176}\text{Yb}/^{177}\text{Hf}^a$	$\pm 2\sigma$	$^{176}\text{Lu}/^{177}\text{Hf}^a$	$\pm 2\sigma$	$^{180}\text{Hf}/^{177}\text{Hf}$	$^{178}\text{Hf}/^{177}\text{Hf}$	$\text{Sig}_{\text{Hf}}^b$ (V)	$^{176}\text{Hf}/^{177}\text{Hf}$	$\pm 2\sigma$	$^{176}\text{Hf}/^{177}\text{Hf}_{(t)}$	$\epsilon\text{Hf}(t)^c$	$\pm 2\sigma$	$T_{\text{DM2}}^d$ (Ga)	age <sup>e</sup> (Ma)
zr8	0.0415	13	0.00141	5	1.88667	1.46716	12.1	0.282872	25	0.282871	3.9	0.6	0.70	18.6
zr7	0.0508	19	0.00176	7	1.88666	1.46722	11.7	0.282890	25	0.282889	4.5	0.6	0.67	18.4
zr6	0.0672	26	0.00297	10	1.88663	1.46709	16.6	0.282839	29	0.282838	2.7	0.8	0.77	18.7
zr2 c	0.0429	30	0.00137	12	1.88668	1.46716	11.3	0.282699	29	0.282692	3.3	0.8	0.95	277
zr3 c	0.0706	22	0.00236	7	1.88657	1.46712	7.5	0.282537	28	0.282497	10.1	0.7	1.09	895
zr8 c	0.0504	21	0.00147	7	1.88663	1.46717	11.3	0.282554	26	0.282530	10.2	0.6	1.05	848
zr9 c	0.0445	34	0.00161	15	1.88661	1.46727	10.1	0.282739	26	0.282731	4.5	0.6	0.88	268
zr4 c	0.0531	52	0.00163	15	1.88655	1.46715	8.3	0.282752	30	0.282744	5.0	0.8	0.85	275
zr5 c	0.0257	15	0.00083	4	1.88667	1.46719	11.6	0.282713	25	0.282709	3.6	0.6	0.92	268
zr12	0.0354	9	0.00120	4	1.88665	1.46719	12.1	0.282826	25	0.282825	2.3	0.5	0.79	18.7
zr14 c	0.0786	46	0.00223	12	1.88651	1.46713	10.1	0.282753	27	0.282743	4.2	0.7	0.87	237
zr15 c	0.0564	13	0.00161	5	1.88659	1.46712	9.1	0.282753	26	0.282745	4.6	0.6	0.86	251
zr13 c	0.0178	17	0.00062	6	1.88654	1.46720	12.3	0.282687	24	0.282684	2.9	0.5	0.97	274
zr13 c	0.0191	33	0.00064	11	1.88675	1.46724	8.4	0.282669	25	0.282666	2.3	0.6	1.00	274
zr1	0.0426	14	0.00145	5	1.88673	1.46719	12.0	0.282847	25	0.282847	3.1	0.6	0.75	18.5
GJ-1 <sup>f</sup>	0.0080	3	0.00029	2	1.88672	1.46717	15.4	0.282003	19	0.282000	-13.8	0.7	2.1	600

<sup>a</sup>  $^{176}\text{Yb}/^{177}\text{Hf} = (^{176}\text{Yb}/^{173}\text{Yb})_{\text{true}} \times (^{173}\text{Yb}/^{177}\text{Hf})_{\text{meas}} \times (M_{173(\text{Yb})}/M_{177(\text{Hf})})^{(H)}$ . The  $^{176}\text{Lu}/^{177}\text{Hf}$  were calculated in a similar way by using the  $^{175}\text{Lu}/^{177}\text{Hf}$ . Quoted uncertainties (absolute) relate to the last quoted figure. <sup>b</sup> Mean Hf signal in volt. <sup>c</sup> calculated using a decay constant of  $1.867 \times 10^{-10}$ , a CHUR  $^{176}\text{Lu}/^{177}\text{Lu}$  and  $^{176}\text{Hf}/^{177}\text{Hf}$  ratio of 0.0332 and 0.282772, and the ages obtained by LA-ICP-MS. <sup>d</sup> two stage model age using the measured  $^{176}\text{Lu}/^{177}\text{Lu}$  of each spot (first stage = age of zircon), a value of 0.010 for the average granitic crust (second stage; Wedepohl 1995), and a depleted mantle  $^{176}\text{Lu}/^{177}\text{Lu}$  and  $^{176}\text{Hf}/^{177}\text{Hf}$  of 0.0384 and 0.28325, respectively. <sup>e</sup>  $^{206}\text{Pb}/^{238}\text{U}$  LA-ICP-MS ages. <sup>f</sup> mean  $\pm 2\sigma$  standard deviation of 9 spot analyses of GJ-1 reference zircon.

Table 2. K-Ar ages obtained on the different igneous rocks of Pohorje Mountains. The age calculation is based on the decay constants given by Steiger & Jäger (1977). The analytical errors are quoted for the 68% confidence levels ( $1\sigma$ ).

Sample	Rock type	Dated fraction	K (%)	$^{40}\text{Ar}$ rad (ccSTP/g)	$^{40}\text{Ar}$ rad (%)	K-Ar age (Ma)
<i>Undeformed dacite</i>						
RD4	dacite	whole rock	2.71	$1.781 \times 10^{-6}$	61.9	$16.8 \pm 0.7$
RD4	dacite	biotite	5.77	$3.870 \times 10^{-6}$	69.3	$17.2 \pm 0.6$
RD4	dacite	biotite	5.94	$3.926 \times 10^{-6}$	93.1	$17.0 \pm 0.4$
MSV1	dacite	biotite	4.67	$2.952 \times 10^{-6}$	66.6	$16.2 \pm 0.7$
RD12	dacite	whole rock	3.06	$1.948 \times 10^{-6}$	57.1	$16.1 \pm 0.6$
JV1	dacite	biotite	5.54	$3.834 \times 10^{-6}$	61.9	$17.7 \pm 0.7$
GP34	dacite	biotite	5.57	$3.485 \times 10^{-6}$	55.6	$16.0 \pm 0.6$
Trb	dacite	biotite	7.05	$4.510 \times 10^{-6}$	68.5	$16.4 \pm 0.5$
MK	dacite	whole rock	2.61	$1.516 \times 10^{-6}$	58.7	$14.9 \pm 0.6$
231	dacite	whole rock	2.74	$1.790 \times 10^{-6}$	71.1	$16.7 \pm 0.5$
233	dacite	whole rock	2.55	$1.668 \times 10^{-6}$	73.7	$16.7 \pm 0.6$
285	dacite	whole rock	2.60	$1.603 \times 10^{-6}$	55.8	$15.8 \pm 0.7$
HK2	dacite	biotite	5.73	$4.039 \times 10^{-6}$	82.2	$18.0 \pm 0.7$
<i>Mafic and deformed dacite dykes</i>						
219	mafic dyke	biotite	3.56	$2.602 \times 10^{-6}$	63.1	$18.2 \pm 0.7$
223	mafic dyke, def.	whole rock	1.17	$8.468 \times 10^{-7}$	63.8	$18.5 \pm 0.7$
223	mafic dyke, def.	biotite	1.79	$1.227 \times 10^{-6}$	44.5	$17.5 \pm 0.7$
232	dacite, de-formed	whole rock	2.05	$1.323 \times 10^{-6}$	74.2	$16.5 \pm 0.5$
232	dacite, de-formed	biotite	2.55	$1.818 \times 10^{-6}$	65.9	$18.2 \pm 0.7$
221	mafic dyke	whole rock	1.76	$1.214 \times 10^{-6}$	78.4	$17.7 \pm 0.7$
221	mafic dyke	whole rock	2.42	$1.558 \times 10^{-6}$	77.9	$16.5 \pm 0.6$
281	mafic dyke, def.	biotite	4.27	$3.090 \times 10^{-6}$	64.1	$18.5 \pm 0.6$
<i>Magmatic pebbles</i>						
332	dacite	biotite	5.67	$4.011 \times 10^{-6}$	84.6	$18.1 \pm 0.6$
338	granodiorite	biotite	6.91	$4.697 \times 10^{-6}$	55.4	$17.4 \pm 0.6$
338	granodiorite	biotite	6.36	$4.116 \times 10^{-6}$	71.3	$16.6 \pm 0.5$
<i>Pohorje pluton</i>						
HK1	gr-porphyre	whole rock	2.66	$1.633 \times 10^{-6}$	74.3	$15.7 \pm 0.6$
HK1	gr-porphyre	biotite	5.65	$3.647 \times 10^{-6}$	62.4	$16.5 \pm 0.7$
RD36	tonalite	biotite	7.65	$5.144 \times 10^{-6}$	78.7	$17.2 \pm 0.7$
216	gr-porphyre	biotite	4.28	$2.931 \times 10^{-6}$	60.6	$17.5 \pm 0.7$
216	gr-porphyre	feldspar	2.35	$1.656 \times 10^{-6}$	65.7	$18.0 \pm 0.7$
221	tonalite	biotite	4.56	$3.053 \times 10^{-6}$	68.9	$17.2 \pm 0.6$
221	tonalite	biotite	4.52	$2.926 \times 10^{-6}$	85.4	$16.6 \pm 0.4$
282	granodiorite	biotite	5.87	$3.883 \times 10^{-6}$	79.0	$16.7 \pm 0.6$
282	granodiorite	biotite	3.32	$2.175 \times 10^{-6}$	66.2	$16.8 \pm 0.5$
282	granodiorite	feldspar	1.34	$9.42 \times 10^{-7}$	68.8	$18.0 \pm 0.6$
280	granodiorite	biotite	6.12	$3.918 \times 10^{-6}$	61.1	$16.4 \pm 0.7$
280	granodiorite	biotite	6.00	$3.911 \times 10^{-6}$	85.8	$16.7 \pm 0.4$
137A	granodiorite	feldspar	1.36	$8.343 \times 10^{-7}$	64.1	$15.7 \pm 0.6$
137A	granodiorite	biotite	6.46	$4.045 \times 10^{-6}$	79.4	$16.1 \pm 0.6$
137A	granodiorite	biotite	6.03	$3.835 \times 10^{-6}$	85.1	$16.3 \pm 0.6$
NV1	tonalite	biotite	4.29	$3.034 \times 10^{-6}$	56.9	$18.1 \pm 0.7$
Nag	granodiorite	biotite	5.79	$3.583 \times 10^{-6}$	62.0	$15.9 \pm 0.5$
137B	cezlakite	biotite	1.63	$1.099 \times 10^{-6}$	53.9	$17.3 \pm 0.7$
137B	cezlakite	amph	0.73	$5.576 \times 10^{-7}$	47.9	$19.5 \pm 0.8$
137B	cezlakite	amph	0.60	$4.751 \times 10^{-7}$	29.3	$20.3 \pm 1.1$
<i>Karawanken-pluton</i>						
Kw	Tonalite	biotite	4.23	$5.376 \times 10^{-6}$	76.7	$32.4 \pm 1.2$

CL-light cores define two age clusters at 200–280 and 850–900 Ma, respectively (Fig. 2c–d). Six concordant to slightly discordant analyses of the first group yielded a concordia age of  $272 \pm 3$  Ma, and, together with the four clearly discordant spots, they define a discordia with an upper intercept age of  $291 \pm 21$  Ma. We consider the concordia age of  $272 \pm 3$  Ma as a minimum age since it is likely that those grains crystallized at 280–290 Ma but experienced some Pb-loss during Miocene magmatism. Therefore, the upper intercept age represents a more conservative estimate for the crystallization age. A common origin of these cores is supported by a rather uniform Hf isotope composition ( $\epsilon\text{Hf}_{(t)} = +2.3$  to  $+5.0$ ), which corresponds to the range of late Variscan ( $\sim 300$  Ma), post-collisional granites in the European basement (e.g., Schaltegger & Corfu, 1992). The  $\epsilon\text{Hf}_{(t)}$  value points to a juvenile source, which could have been either young crust with an average Neoproterozoic Hf model age, slightly younger than that of the early Neoproterozoic cores (Fig. 2e), or a mixture of a mantle-derived and a crustal component. The  $\epsilon\text{Hf}_{(t)}$  values of the two early Neoproterozoic cores (Fig. 2d) is close to the depleted mantle composition at that time (Fig. 2e). Miocene CL-dark domains have  $\epsilon\text{Hf}_{(t)}$  values of  $+2$  to  $+4$ . Assuming that a crust represented by the Permian and Neoproterozoic cores evolves with an average  $^{176}\text{Lu}/^{177}\text{Hf}$  ratio of 0.010 (Wedepohl et al. 1995) its Miocene  $\epsilon\text{Hf}_{(t)}$  value would plot just below that of the Miocene overgrowth domains (grey field with white S in Fig. 2e). Thus an additional juvenile component, such as a juvenile Phanerozoic crustal component or a Miocene mantle-derived melt (see grey arrows in Fig. 2e), must have been involved as a source of the magma in order to explain its Hf isotope composition.

#### K-Ar data

K-Ar dating has been performed by the conventional method using high frequency induction heating and getter materials (titanium sponge and SAES St707) for extracting and cleaning the argon. The potassium was determined by flame photometry using a CORNING 480 machine. Details of the analytical techniques and the results of calibrations have been described by Balogh (1985) and Odin et al. (1982). The results of the K-Ar isotopic dating on mono-mineralic fractions and whole rock samples are given in Table 2 and shown in Figures 1a and b. A detailed discussion of K-Ar data is found in Trajanova et al. (2008).

Biotite ages from the pluton range from  $18.1 \pm 0.7$  to  $15.9 \pm 0.5$  Ma ( $\pm 1\sigma$ ) (Fig. 1b). They are considered to record cooling below the closure temperature of biotite. Feldspar and whole rock isotope ages scatter between  $18.0 \pm 0.7$  and  $15.7 \pm 0.6$  Ma and fit well with the biotite ages. In two samples (216 and 282) feldspar fractions show somewhat older ages than biotite, but the ages overlap within error limits (Table 2). Two amphibole fractions from a small gabbroic body in the old Cezlak quarry (site 137B) yielded K-Ar ages of  $20.3 \pm 1.1$  Ma and  $19.5 \pm 0.8$ . These are basically in agreement with the obtained U-Pb isotope age. The biotite age ( $17.3 \pm 0.7$  Ma) ob-

tained from this site corresponds to those determined from tonalitic and granodioritic lithologies of the pluton. Biotite ages from one foliated and one nearly undeformed granodiorite pebble found in the eastern part of the Ribnica-Selnica trough (site 338) are consistent with the ages of intrusion.

Dacitic and mafic dykes exhibiting traces of ductile deformation (referred to as “deformed dykes” in the following) and undeformed mafic dykes show biotite ages between  $18.5 \pm 0.6$  and  $17.5 \pm 0.7$  Ma (Table 2, Fig. 1b). Whole rock ages from these dykes range between  $18.5 \pm 0.7$  and  $16.5 \pm 0.5$  Ma.

Biotite ages from shallow intrusive dacite bodies and undeformed dykes range from 18.0 to 16.0 Ma, whereas whole rock ages yielded slightly younger ages varying from 16.8 to 14.9 Ma (Table 2., Fig. 1b). The oldest biotite age of  $18.1 \pm 0.6$  Ma was obtained from a rhyodacite pebble (site 332, Fig. 1b), which was derived from a surface lava flow.

#### Fission track data

The results of zircon fission track analyses on five samples from the Pohorje pluton and dacite dykes are listed in Table 3 and shown in Figure 1b. Sample preparation techniques, details of the method and instruments applied are the same as those described by Dunkl et al. (2001). The three FT analyses from the dacites consistently yielded ages around 17.5 Ma. These ages are slightly older than those from the tonalite (16.9 and 15.6 Ma). In the case of tonalite sample 280 the chi-square test failed (Green, 1981). Together with the high dispersion (Galbraith & Laslett, 1993), this indicates that the single grain ages do not follow a Gaussian distribution (Table 3).

#### Petrology and mineral chemistry

Two samples from the eastern (sample 311) and western (sample 216) part of the Pohorje pluton (Fig. 1) were analyzed with the electron microprobe in order to compare mineral chemistries (Table 4) and to obtain data for thermobarometric calculations. For the instrumental details and correction procedures applied, see Balen et al. (2006).

Both analysed samples contain the same mineral assemblage of amphibole, biotite, plagioclase, K-feldspar, quartz and accessories. No chemical zonation is found within the analysed grains, but some variation exists amongst the individual grains (Table 4). Following the classification of Leake et al. (1997), all amphiboles from sample 216 fall into the magnesiohornblende field, whereas amphiboles from sample 311 are at the boundary between tschermakite and ferro-tschermakite. The investigated tonalites contain the mineral assemblage required for the application of the Al-in-hornblende barometer. We used the calibrations of Hammarstrom & Zen (1986), Hollister et al. (1987) and Schmidt (1992). All three calibrations yielded pressure estimates with a fairly acceptable error range (mostly 0.5 kbar). For sample 216 we calculated 3 to 4 kbar, while sample 311 formed at pressures of about 6–7 kbar. This corresponds to crustal depths of some 8–11 km and 16–19 km, respectively. The higher pressure obtained from sample 311 is in good agreement with previous pressure estimates of  $6.8 \pm 0.4$  kbar by Altherr et al. (1995), who also investigated samples originating from the eastern Pohorje pluton (Cezlak, site 137A, Fig. 1). However, further data are needed to confirm the difference in crystallization depth between the eastern and western segment of the Pohorje pluton. From these pressure values, temperatures were estimated with the method of Blundy & Holland (1990). Sample 216 yielded 750–770 °C, while for sample 311 somewhat higher temperatures of 760–820 °C were calculated.

#### Deformation of the igneous rocks

##### Syn-magmatic deformation

Tonalites and granodiorites that were only weakly affected by solid-state deformation often show a foliation defined by the preferred alignment of biotite and the long axes of amphibole grains. Therefore, this foliation seems to have developed during the magmatic stage. Some dacitic dykes show well-developed magmatic flow fabrics at the micro scale.

Two main generations of dykes occur near the Pohorje pluton. A first generation (Fig. 3a) consists of aplites and de-

Table 3. Zircon fission track data obtained on the igneous rocks of Pohorje Mountains.

Sample	Lat. Nord	Long. East	Lithology	Cryst.	Spontaneous		Induced		Dosimeter		P( $\chi^2$ ) (%)	Disp.	FT age* (Ma $\pm$ 1s)
					rs	(Ns)	ri	(Ni)	rd	(Nd)			
RD12	46° 32.2'	15° 10'	dacite	20	53.3	(618)	134.1	(1555)	6.89	(4543)	58	0.02	17.5 $\pm$ 0.9
RD4	46° 32.5'	15° 08'	dacite	20	48.6	(731)	121.4	(1826)	6.92	(4543)	22	0.07	17.7 $\pm$ 0.9
285	46° 29.2'	15° 11'	dacite	19	57.6	(669)	145.5	(1776)	6.99	(4543)	41	0.02	17.7 $\pm$ 0.9
RD36	46° 31.5'	15° 15'	tonalite	20	54.9	(702)	144.7	(1849)	6.95	(4543)	27	0.06	16.9 $\pm$ 0.8
280	46° 29.8'	15° 20'	tonalite	20	63.4	(1041)	117.4	(1928)	4.54	(8928)	0	0.19	15.6 $\pm$ 0.9

Cryst.: number of dated zircon crystals.

Track densities (p) are as measured ( $\times 10^5$  tr/cm<sup>2</sup>); number of tracks counted (N) shown in brackets.

P( $\chi^2$ ): probability obtaining Chi-square value for n degree of freedom (where n = no. crystals – 1).

Disp.: Dispersion, according to Galbraith and Laslett (1993).

\* Central ages calculated using dosimeter glass: CN 2 with  $\zeta = 127.8 \pm 1.6$ .

Table 4. Representative mineral chemical data of the Pohorje tonalites, used for thermobarometric calculations from sites 216 and 311.

<b>Amphibole</b>					<b>Plagioclase</b>					<b>Biotite</b>				
Sample	Slo-216		Slo-311		Sample	Slo-216		Slo-311		Sample	Slo-216	Slo-311		
SiO <sub>2</sub>	44.79	44.13	40.86	41.81	SiO <sub>2</sub>	61.01	60.92	60.56	61.54	SiO <sub>2</sub>	36.56	36.70		
Al <sub>2</sub> O <sub>3</sub>	8.26	10.73	12.58	11.19	Al <sub>2</sub> O <sub>3</sub>	24.70	24.28	24.21	24.50	Al <sub>2</sub> O <sub>3</sub>	14.49	14.55		
TiO <sub>2</sub>	1.19	1.58	1.07	0.93	CaO	6.25	6.24	6.59	6.69	TiO <sub>2</sub>	3.61	2.57		
FeO	16.30	13.60	19.90	20.68	Na <sub>2</sub> O	8.21	7.62	7.82	7.49	FeO	17.99	20.36		
MnO	0.78	0.71	1.06	0.74	K <sub>2</sub> O	0.33	0.27	0.27	0.27	MnO	0.43	0.45		
MgO	12.35	12.25	7.78	7.65	Total	100.51	99.33	99.45	100.49	MgO	11.65	10.82		
CaO	11.42	11.84	11.28	11.67	<i>cation numbers on the basis of 8 O</i>				CaO	0.20	0.00			
Na <sub>2</sub> O	1.45	1.22	1.59	1.43	Si	2.703	2.722	2.711	2.720	Na <sub>2</sub> O	0.17	0.00		
K <sub>2</sub> O	0.68	0.57	1.50	1.33	Al	1.290	1.279	1.277	1.276	K <sub>2</sub> O	9.50	9.50		
Total	97.22	96.63	97.62	97.43	Ca	0.297	0.299	0.316	0.317	Total	94.61	94.94		
<i>cation numbers on the basis of 23 O</i>					Na	0.705	0.660	0.679	0.642	<i>cation numbers on 22 O</i>				
Si	6.608	6.505	6.203	6.393	K	0.019	0.015	0.015	0.015	Si	5.610	5.663		
Al <sup>IV</sup>	1.392	1.495	1.797	1.607	An	29.07	30.66	31.29	32.53	Al	2.620	2.646		
Fe <sup>3+</sup>	0.000	0.000	0.000	0.000	<b>K-feldspar</b>					Ti	0.416	0.298		
T	8.000	8.000	8.000	8.000	<b>Sample</b>			<b>Slo-216</b>		<b>Slo-311</b>		Fe <sup>2+</sup>	2.308	2.627
Al <sup>VI</sup>	0.044	0.369	0.454	0.410	SiO <sub>2</sub>	63.90	63.74	Al <sub>2</sub> O <sub>3</sub>	17.56	18.64	Mn	0.056	0.059	
Ti	0.132	0.175	0.122	0.107	BaO	0.65	1.99	Na <sub>2</sub> O	0.97	0.91	Mg	2.664	2.488	
Fe <sup>3+</sup>	0.930	0.580	0.669	0.476	K <sub>2</sub> O	15.51	14.93	Total	98.59	100.21	Ca	0.033	0.000	
Mg	2.716	2.691	1.761	1.743	<i>cation numbers on 8 O</i>					Na	0.050	0.000		
Fe <sup>2+</sup>	1.081	1.096	1.858	2.168	Si	3.009	2.971	Al	0.974	1.024	K	1.859	1.870	
Mn	0.097	0.089	0.136	0.096	Ba	0.012	0.036	Na	0.089	0.082	Total	15.618	15.651	
C	5.000	5.000	5.000	5.000	Na	0.089	0.082	K	0.931	0.888				
Mn	0.000	0.000	0.000	0.000										
Ca	1.805	1.870	1.835	1.912										
Na	0.195	0.130	0.165	0.088										
B	2.000	2.000	2.000	2.000										
Na	0.220	0.219	0.303	0.336										
K	0.128	0.107	0.290	0.259										
A	0.348	0.326	0.593	0.595										
Total	15.665	15.521	15.823	15.758										

formed mafic and dacite dykes that trend E–W to NW–SE, with gentle to moderate dips; this generation is oriented sub-parallel to the foliation of the host metamorphic rocks (Fig. 3). Emplacement was probably controlled by the pre-existing foliation. A second generation (Fig. 3b) consists of undeformed mafic and dacite dykes with trend between NNW–SSE and NNE–SSW; only a very few vertical dykes trend WNW–ESE. The dominant set is vertical or steeply dipping and can be interpreted as tensional cracks or conjugate extensional shear fractures. These formed in an ~E–W oriented extensional regime.

#### Solid-state deformation

The rocks of the Pohorje pluton show clear evidence for solid-state deformation after magmatic crystallization. Where the foliation is well developed, it totally overprints the magmatic fabric. Alignment of biotite and amphibole crystals and elongated lenses of quartz and feldspar locally define a weak stretching lineation. In the northeastern part the foliation is steeply to moderately dipping and is either sub-parallel or at a small angle to the pluton margin (Figs. 1a, 4). The lineation is mostly gently

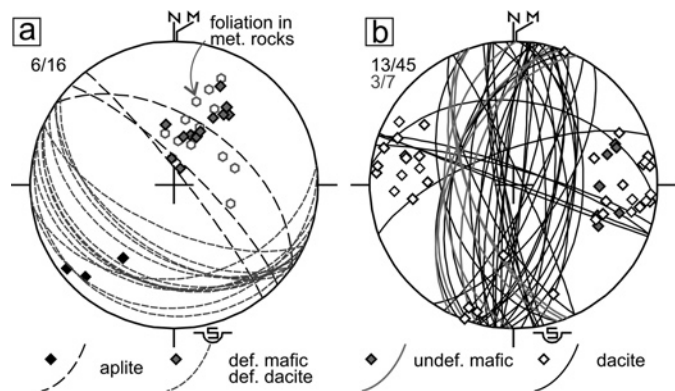


Fig. 3. Stereographs of dykes in the surroundings of the Pohorje pluton; lower hemisphere projection, Schmidt net. Numbers in upper left corner indicate the number of sites and measurements, respectively. 3a: aplite and deformed dykes 3b: undeformed dacite and mafic dykes

dipping. In the southwestern part, the foliation is mainly gently dips to the SE or WSW, partly being sub-parallel to the undulating pluton boundary (Figs. 1a, 4). The lineation mainly trends E–W, being oriented oblique or down dip within the foliation.

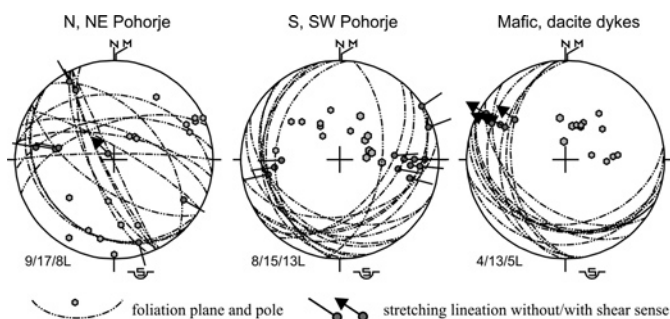


Fig. 4. Stereographs showing the orientations of ductile fabrics found within two domains the Pohorje pluton, and within deformed mafic and dacite dykes. Numbers in lower left corner indicate the number of sites, foliation planes, lineations, respectively.

The scatter in the orientation of the foliations is at least partly due to later deformation.

At the micro scale, solid-state deformation is best evidenced by the complete dynamic recrystallization of quartz into elongated lenses within the most heavily deformed samples (Fig. 5a). Primary biotite was sheared and partly recrystallised into highly elongated, fine-grained tails along the foliation (Fig. 5b). Feldspars mostly show brittle behaviour, but deformation twins, bent twins and incipient core-mantle structures indicate crystal plastic deformation. In the more deformed rocks biotite and quartz tend to form interconnected weak layers, and a typical “augengneiss” structure is developed. In less deformed rocks quartz is partly recrystallised, the relict grains show intensive undulous extinction and formation of subgrains. The microstructural features indicate deformation temperatures characteristic of medium to high-T greenschist facies. This is in accordance with the observation that biotite is generally stable during deformation and transformed into chlorite only to a small extent.

Mafic xenoliths in the tonalite are strongly flattened due to vertical shortening (Fig. 5c). Subvertical aplite dykes suffered folding with gently dipping axial planes. In the Cezlak quarry (site 137A) several moderately E and W dipping ductile shear zones are exposed and form conjugate pairs. They offset aplitic and pegmatitic dykes with a normal sense of shear, and are characterized by grain-size reduction due to incipient mylonitisation (Fig. 5d).

The deformed dacitic or mafic dykes show incipient stages of ductile deformation, mainly along their margins. Their foliation is sub-parallel to the foliation in the host metamorphics (Fig. 4). Site 232 exhibits a penetrative foliation (Fig. 5e), and a weak stretching lineation defined by elongate minerals developed. The shape preferred orientation in dynamically recrystallised quartz aggregates indicates top-to-WNW shear (Fig. 4).

Altogether, our observations demonstrate that the whole Pohorje pluton as well as some related dyke rocks underwent solid state deformation in the upper greenschist facies following the emplacement and crystallisation. This indicates that cooling and uplift was triggered by active tectonics, resulting

in vertical flattening associated with ca. E–W stretching mostly, whereas the formation of moderately to steeply dipping foliation with gently dipping lineation in the northeastern part of the pluton is not yet understood.

#### Brittle deformation

We analyzed brittle deformation by fault-slip analysis and determination of paleostress tensors (Angelier 1984), by observation of cross-cutting relationships in outcrops, and by reinterpretation of map-scale structures. Most of the brittle faults belong to a transtensional deformation phase. Normal faults, trending from NW–SE to NNE–SSW are the most characteristic structural elements both in outcrop- and map scales. The symmetry plane of conjugate normal fault pairs is often not vertical (site 231 on Fig. 6), which indicates a tilting during normal faulting. Normal faults show gradual transition to oblique-normal or even pure conjugate strike-slip faults; sites 137B and 300 show typical examples (Fig. 6).

N–S trending faults displace the southern margin of the pluton at several locations (Fig. 6). NW–SE striking normal or oblique-normal faults bound dacite bodies in the NW Pohorje Mountains, and also the western margin of the Ribnica-Selnica trough. At the eastern margin of the Pohorje Mountains oblique-normal faults are postulated between the metamorphic rocks and the Triassic to Miocene sediments (Fig. 6). Observed syndimentary normal faults in the areas immediately west and south of Pohorje (Fodor et al. 1998) clearly demonstrate that the E–W tensional phase was associated with Early to Middle Miocene extensional opening of the Pannonian basin and has lasted throughout Middle Miocene.

As typical for transtensional stress field, the calculated stress tensors mostly shows extensional characters, but few sites are marked by strike-slip type stress field with N–S compression. In all cases, the  $\sigma_3$  stress axes are horizontal, and vary from SW–NE to ESE–WNW, with a prevailing E–W direction. This dispersion of orientations probably reflects spatial variations of the stress field. Extensional and strike-slip type stress tensors show transition, because (1) stress axes  $\sigma_2$  and  $\sigma_1$  are similar in value, (sites 137B and 300 on Fig. 6) and (2) strike-slip faults show only minor misfit with respect to the extensional stress tensor.

A few sites in the northern part of the pluton exhibit conjugate strike-slip faults and hence are characterised by a strike-slip type stress field, with a horizontal  $\sigma_1$  axis trending NE to E (Fig. 6b). These structures represent a separate deformation phase whose importance is minor on map-scale fault pattern. This phase could follow the transtensional deformation (with E–W extension) as a short transient episode at around the Middle to Late Miocene boundary (late Sarmatian to early Pannonian) by using analogies from the Pannonian basin and Eastern Alps (Peresson & Decker 1997; Fodor et al. 1999; Pischinger et al. 2008).

A third deformation phase is characterized by a conjugate set of strike-slip and reverse faults (Fig. 6c). Dextral slip oc-

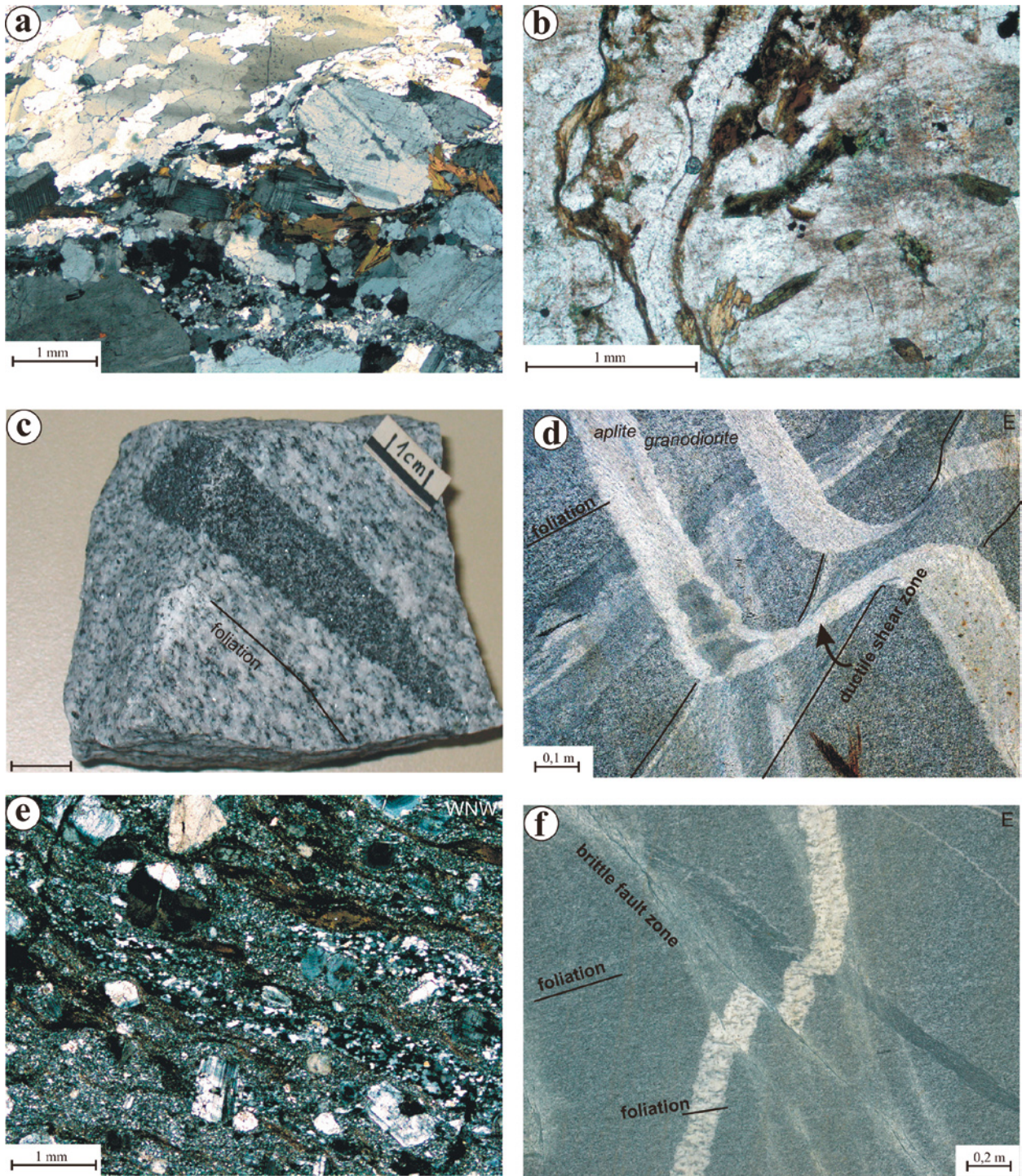


Fig. 5. Solid-state deformation of the Pohorje pluton and related dykes. 5a: Photomicrograph of a foliated medium-grained tonalite (sample 311). Note the complete dynamic recrystallisation of quartz (upper left) and fine-grained, newly formed feldspars (mirmekite) along the grain boundaries of larger K-feldspars (lower central). +N. 5b: Deformation of biotite: primary magmatic crystals are surrounded by very elongate, anastomosing, sheared and recrystallised tails which form interconnected weak layers defining the foliation (subvertical) with dynamically recrystallised quartz ribbons. Idiomorphic prismatic crystals at the right are amphiboles. Sample 216, 1N. 5c: Hand specimen of a well-foliated granodiorite with an elongate mafic enclave oriented subparallel to the foliation. SE Pohorje, Cezlak quarry (137A). 5d: Steeply dipping, leucocratic dyke crosscutting foliated granodiorite from Southeastern Pohorje, Cezlak quarry, site 137A. The dykes are cut by a ductile shear zone. 5e: Photomicrograph of a strongly deformed dacite dyke from the western Pohorje (site 232). Note well-developed foliation defined by elongated, dynamically recrystallised quartz ribbons and aligned “biotite-fishes” with strongly elongated, recrystallised tails. +N. 5f: Subvertical, leucocratic dyke crosscutting foliated granodiorite and a mafic enclave. The dyke is also flattened vertically, as is indicated by the same, gently dipping foliation observed in the host granodiorite. Note also late, brittle normal faults with decimetre-scale offsets. SE Pohorje, Cezlak quarry (137A).

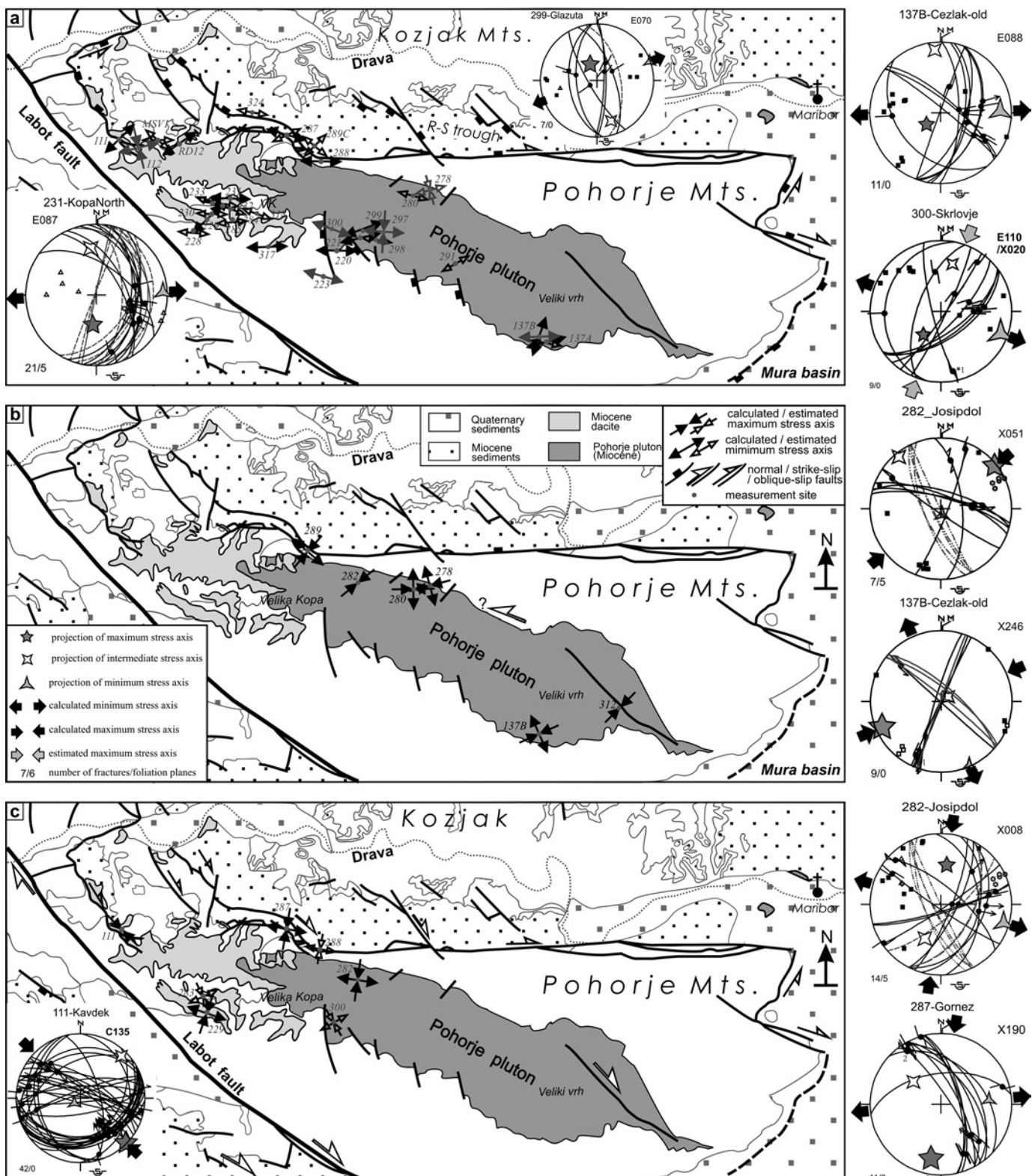


Fig. 6. Fault-slip data, stereographic projections of fractures and paleostress axes calculated with the software of Angelier (1984). For pre-Miocene formations, see Figure 1. Numbers in upper right corner show the stress type: C for compression, X for strike-slip, E for extension with the direction of  $\sigma_1$  and  $\sigma_2$  axes (for C, X and E, respectively). 6a: Transtensional phase with ~E-W extension and locally with ~N-S compression. Note tilted fractures at site 231. Grey arrows indicate axes of a stress state being close to strike-slip type stress. 6b: Strike-slip faulting associated with NE-SW to E-W compression. 6c: Strike-slip faulting associated with N-S compression.

curred along the Lavanttal-Labot fault, along other NW–SE trending faults of the NW Pohorje area, and also along the western margin of the Ribnica-Selnica trough. Dextral faulting is suggested in the eastern Pohorje pluton along the fault bounding the narrow metamorphic belt although kinematics is not directly confirmed. The calculated compressional axis is between NNW–SSSE and NNE–SSW, while the tensional axis is perpendicular (Figs. 6c). These strike-slip faults are younger, because (1) they often reactivate normal faults of the E–W extension, proved by relative chronology between dip-slip and strike-slip striae, and (2) because subvertical NW–SE trending dextral faults cut eastward-dipping normal faults north from the Pohorje, in the Kozjak area. The occurrence of strike-slip faulting, combined locally with transpressional deformation, is characteristic for the Late Miocene to Quaternary structural evolution of the wider area (Fodor et al. 1998; Márton et al. 2002; Sölvá et al. 2005; Vrabec et al. 2006).

## Discussion

### *Age of emplacement of the Pohorje pluton and related magmatic rocks*

The new U-Pb data demonstrate a late Early Miocene age of emplacement ( $18.64 \pm 0.11$  Ma) of the Pohorje pluton. This age is markedly different from the Oligocene isotopic ages typically obtained for the Periadriatic plutons (von Blanckenburg and Davies 1995). The age difference is particularly striking in comparison with the nearest Periadriatic intrusion, the Karawanken tonalite, for which we obtained a K-Ar biotite age of  $32.4 \pm 1.2$  Ma (Fig. 1b, Table 2; Trajanova et al. 2008), in agreement with previous data (Scharbert 1975, Elias 1998). The Karawanken and Pohorje intrusions also show considerable differences in terms of their geochemical character and inferred magma sources; the Pohorje pluton is relatively more enriched in large ion lithophile elements (LILE) as well as in La, Ce and is hence interpreted as the product of partial melting of amphibolite and eclogite (Zupančič 1994b; Benedek & Zupančič 2002; Márton et al. 2006). Therefore, the Pohorje pluton is not part of the Oligocene-age Periadriatic intrusive suite, as was previously suggested by numerous authors (e.g. Laubscher 1983; Elias 1998; Pamić & Pálinkáš 2000; Pálinkáš & Pamić 2001; Rosenberg 2004). Moreover, the new U-Pb age is in agreement with the Miocene age postulated for this pluton by other authors (Deleon 1979; Dolenc 1994; Altherr et al. 1995; Trajanova et al. 2008).

The oldest K-Ar ages (19.5–20.3 Ma) are obtained on amphiboles from a small gabbroic inclusion within the southeastern Pohorje pluton. These ages are very close (within  $1\sigma$  error) to the U-Pb age (18.64 Ma) for the Pohorje pluton and in accordance with the assumption that the gabbro crystallized during the early phase of magma evolution.

The average ages obtained from deformed dacite and mafic dykes are slightly younger (18.5–18.2 Ma) than the U-Pb age of the pluton and appear to be older than biotite ages and zircon

fission track ages from the dacite. Although the K-Ar ages overlap within the  $1\sigma$  error range, the paleomagnetic data (Márton et al. 2006) suggest a relatively older formation of deformed dacite and mafic dykes, since they record one additional rotational event in comparison with the dacites.

Regarding the dacite bodies, the biotite K-Ar and the zircon fission track ages are very similar (18–16 and 17.7–15 Ma, respectively). The mean values are close to the assumed age of the Karpatian sediments that also contain pyroclastic intercalations (17.3–16.5 Ma, Steininger et al. 1988). Therefore, we interpret the biotite K-Ar ages and the zircon fission track ages from the undeformed dacites to be close to the emplacement age of the dacites. Dacite magmatism may have already started in the Ottnangian, as is indicated by the oldest biotite ages around 18 Ma, including the age from the rhyodacite pebble. The youngest dacite intrusions occur within Karpatian sediments. The biotite K-Ar age of the Vuzenica body ( $16 \pm 0.6$  Ma, sample GP-34 in Fig. 1b) and the slightly younger apatite fission track age (15 Ma; Sachsenhofer et al. 1998) constrain the age of termination of the magmatic activity as early Middle Miocene.

The total time span inferred for the Pohorje magmatism (about 18.5–16 Ma) corresponds to important pulses of volcanism found in the Pannonian Basin system. The oldest Miocene magmatic suite, the so-called “lower rhyolite tuff” has an Ottnangian stratigraphic age (Hámor 1985); the K-Ar mean age was considered to be  $19 \pm 1.4$  Ma for a long time (Hámor et al. 1987; Pécskay et al. 2006). However, new U-Pb and Ar-Ar data from two sites suggest that part of the suite may be as young as 17 Ma (Pálffy et al. 2007). Latest Early to early Middle Miocene igneous activity is well demonstrated in the Styrian basin, located some 20–40 km NE of the Pohorje Mountains in Austria (Ebner & Sachsenhofer 1991). There the age of volcanism (17.3–15 Ma) is constrained by intercalated Karpatian to earliest Middle Miocene marine sediments. Contemporaneous volcanic events produced the so-called “middle rhyolite horizon”, a dacitic-rhyodacitic suite in the Pannonian Basin (Harangi et al. 2005). Despite this temporal coincidence, the geodynamic settings of all these magmatic suites may possibly be different.

### *Cooling history and exhumation of the Pohorje pluton*

#### Magmatic rocks

Our thermo-chronological data permit the reconstruction of the cooling history of the magmatic rocks in the Pohorje Mountains (Fig. 7). The biotite K-Ar ages from the pluton are noticeably younger than its U-Pb age, suggesting that they record cooling and synchronous solid-state deformation of the pluton. Zircon fission track ages are still younger than biotite age from the same sites and thus record a further step along the cooling path. Feldspar ages fit into the general trend of the cooling history although scattered ages may reflect a somewhat disturbed isotope system. Biotite cooling ages from granodior-

rite pebbles are identical with the postulated Karpatian age of the host sediment (within limits of error), which also indicates rapid exhumation and denudation of the pluton. Considering the youngest biotite and FT ages, as well as the age of the sediments, the entire cooling process below the annealing temperature of fission tracks in zircons must have occurred within 3 Ma (18.6–15.6 Ma).

### Metamorphic rocks

Several K-Ar ages were reported from the metamorphic host rocks of the Pohorje and Kozjak Mountains (Fodor et al. 2002b). A detailed discussion of these ages is beyond the scope of this paper and we only briefly consider data that are relevant for inferring the exhumation history of the Pohorje pluton. With one exception, the white mica and biotite K-Ar ages from the host rocks are within the 30–13 Ma range and at least partly reflect the thermal effect from the Pohorje intrusives and possibly that of other buried and unexposed magma bodies (Fig. 1a). This is clearly shown by the existence of thermally “undisturbed” Eoalpine (Cretaceous) mica ages reported from the Kozjak Mountains (except for its eastern portion), as well as by the Cretaceous ages obtained from high-T retentivity isotopic data for the metamorphic rocks in the Pohorje Mountains (Thöni 2002; Miller et al. 2005; Janák et al. 2007). Amphibole K-Ar ages >100 Ma from both the Pohorje and the Kozjak Mountains indicate no resetting (Fig. 1a). One white mica age (102 Ma) from the southernmost Pohorje Mountains, as well as two illite ages from the Kozjak Mountains, which derive from the weakly metamorphosed Upper Austroalpine Paleozoic rocks, are considered as undisturbed Cretaceous cooling ages of the Eoalpine metamorphic event.

The K-Ar white mica ages from the metamorphic rocks reflect a younging trend from west to east (Fig. 1a). In the western part, the muscovite ages, and the zircon fission track ages, are Oligocene and therefore older than the granodiorite intrusion itself; only one biotite age (from close vicinity to the pluton; site 222) is identical with the magmatic biotite ages. These Oligocene ages suggest that the western part of the metamorphic host rocks were cooled below the closure temperature of muscovite (ca. 350 °C) and possibly also below the annealing temperature of the zircon fission tracks (ca. 250 °C) prior to magmatism and were not substantially reheated by the pluton (Fig. 7, cooling path A). Ages from the medium-grade metamorphic rocks in the central southern and northern Pohorje Mountains (sites 271–273, 138) are close to those obtained for the magmatic rocks, and they thus indicate a common cooling history (cooling path B on Fig. 7). While the muscovite and biotite ages in the metamorphic rocks of the easternmost Pohorje Mountains are consistently younger than the biotite age from the pluton, this demonstrates that this part underwent later cooling (Fig. 7, path C). Biotite cooling ages from the pluton itself, however, do not show a similar trend, suggesting that the K-Ar system in biotite was uniformly affected by heat derived from magmatism.

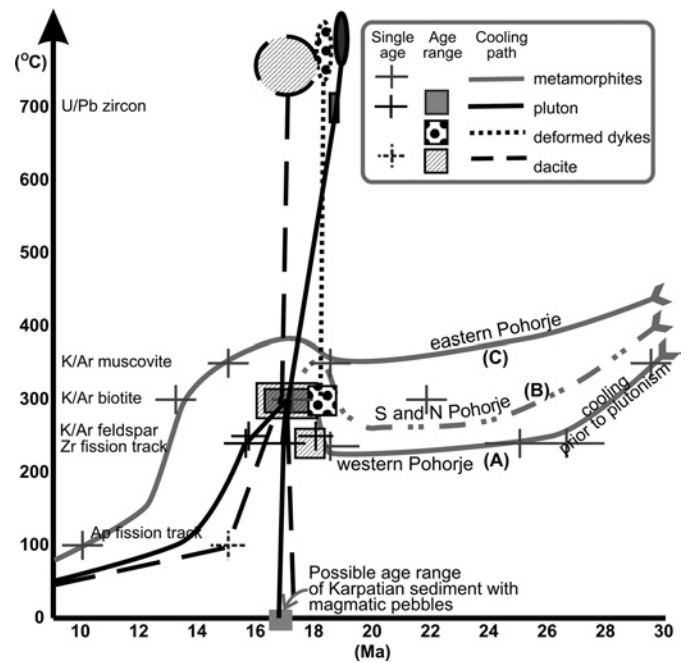


Fig. 7. Cooling history of the Pohorje pluton and surrounding metamorphic rocks. Crosses and boxes indicate the ranges of error concerning age (horizontally) and closure temperature (vertically, and only schematically).

### Summary of the emplacement and cooling of the Pohorje pluton

A simplified summary on the evolution of the Pohorje pluton itself, related other magmatic activity and that of the surrounding metamorphic host rocks is shown in Fig. 8. The emplacement of the pluton occurred at 18.6 Ma, as indicated by our U-Pb isotope age data. Inherited zircon cores of Permian and Neoproterozoic age point to melting and/or assimilation of crustal material with Neoproterozoic Hf model ages. The Hf isotope composition of Miocene zircon domains suggests involvement of a juvenile Phanerozoic crust or a Miocene-age mantle-derived melt as a source of the magma. Limited thermobarometric data suggest a relatively larger crystallization depth in the east compared to the west, where the intrusion of the pluton almost reached the weakly metamorphosed Austroalpine unit.

The magma intruded medium-grade metamorphic rocks, which previously underwent Cretaceous (Eoalpine) metamorphism and ductile deformation (Fig. 8a). Fodor et al. (2002a) and Trajanova (2002) demonstrated examples of extensional shear zones, which form an important detachment zone at the top of the medium-grade rocks. By Miocene times, these rocks were already cooled below the closure temperatures of amphibole, and, at least in the western Pohorje Mountains, below the closure temperature of muscovite. On the other hand, advective heat transfer from the magmatic intrusion in the northern, southern and eastern Pohorje area reheated the host metamorphic rocks.

Just after its emplacement, at ~18.5–18.2 Ma, the pluton was cut by aplitic and mafic dykes, which partly intruded into host metamorphic rocks along the pre-existing foliation (Fig. 8b). The pluton shows magmatic flow structures, which, however, are difficult to separate from overprinting solid-state deformation. Solid-state deformation occurred during fast cooling of the pluton, probably under greenschist facies conditions and before cooling below the closure temperature of biotite at around 17.1–16.5 Ma. The subhorizontal foliation planes and E–W mineral lineations in the southwestern part of the pluton indicate vertical flattening and E–W stretching while the moderately to steeply dipping foliation with gently dipping lineation in the northeastern pluton reflect a different type of deformation, probably strike-slip faulting (Fig. 8c).

The emplacement of the dacite stock started at around 18 Ma, and rhyodacitic lava flows also formed at that time (Fig. 8c). Because of the shallow intrusive level, cooling was fast, and hence, no ductile deformation feature was observed. Dykes were emplaced into the westernmost parts of the pluton and both into the medium- and low-grade metamorphic rocks, crosscutting earlier formed detachment zones. N–S trending dacite dykes were presumably controlled by extensional deformation, although the interpretation of WNW trending vertical dykes needs further consideration.

Dacite volcanoclastics were intercalated with sediments during the Karpatian (17.3–16.5 Ma), and dacite magmatism ended during the early Middle Miocene, i.e. around 16 Ma (Fig. 8d). Pebbles were eroded from both the pluton and dacite suites and transported into the Karpatian sedimentary basin. The entire geochronological data set and the presence of magmatic pebbles in Karpatian sediments demonstrate rapid cooling of the pluton after its emplacement through the temperature range typical for ductile deformation and below the annealing temperature of the zircon fission tracks, partly even all the way to the surface within only some 3 Ma.

This process was associated with ductile to brittle deformation of the pluton itself, some of the dykes and the older parts of the dacite bodies (Fig. 8d). Magmatic and solid-state fabrics of the pluton were cut by ductile shear zones and brittle faults, and tilted around horizontal axes. Fault pattern and stress calculations suggest that this deformation phase had a transtensional character, where normal and strike-slip faults were active. In the southwestern part of the pluton, the direction of brittle extension and the orientations of the ductile lineations are parallel to each other, suggesting persistent extensional deformation during ongoing cooling, while strike-slip type deformation could prevail in the NE. Older K–Ar muscovite ages in the host rocks, smaller crystallisation depth, and the close position of weakly metamorphosed uppermost Austroalpine unit with respect to the pluton could all confirm a relatively smaller amount of exhumation in the western part of the Pohorje Mountains.

The activity of brittle E–W extension, locally combined with N–S strike-slip faulting, conforms with lateral tectonic extrusion (a combination of orogenic collapse and continental escape), which affected the whole Eastern Alps in Early to

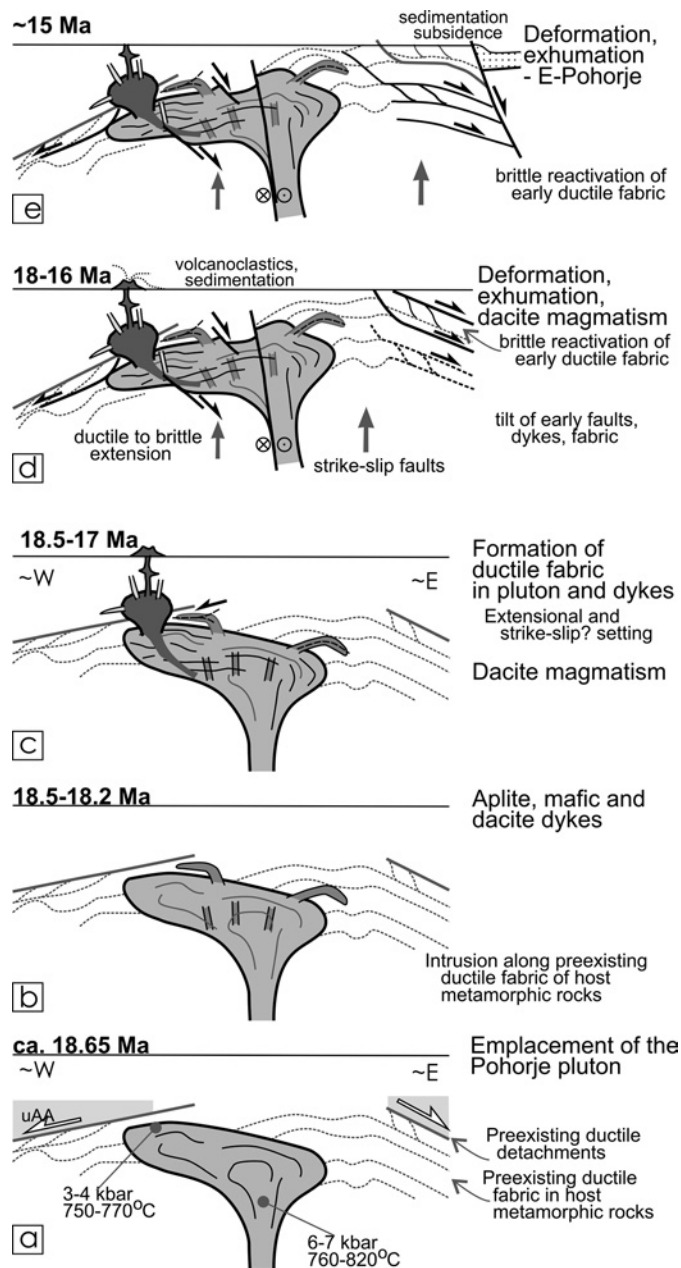


Fig. 8. Sketch for the evolution of the Pohorje pluton and surrounding rocks in terms of a series of ~E–W oriented cross sections. Age ranges are overlapping because some processes were coeval and/or the applied dating methods are not precise enough to separate distinct events. Uppermost weakly metamorphosed units are marked by uAA.

Middle Miocene times (Ratschbacher et al. 1991, Frisch et al. 1998, 2000). Similar data are reported from the northern vicinity of the Pohorje Mountains, in the Koralm region (Pischinger et al. 2008). Frisch et al. (1998, 2000) and Dunkl et al. (2003) showed that an important extensional pulse accelerated E–W extension for a short period of time around 17 Ma. The 18–17 Ma time span also corresponds to the first and most significant lithospheric extensional event of the adjacent Pannonian

Basin, where high rates of subsidence occurred just east of the Pohorje Mountains, in the Mura-Zala basin (Tari et al. 1992; Sachsenhofer et al. 2001; Márton et al. 2002). In the Pohorje Mountains, this type of deformation was already active from at least 17 Ma onwards, when the pluton and most of the host metamorphics cooled below ca 300–250 °C. If the ductile fabric formed by the same type of deformation, this would indicate the onset of this phase about 1 Ma earlier, in agreement with the briefly mentioned regional data.

The next stage in the exhumation occurred at around 15–13 Ma and in the eastern Pohorje Mountains, as is documented in the area east of the pluton (Fig. 8e). Pre-existing ductile shear zones were reactivated and resulted in tectonic exhumation. Formation of the western boundary fault of the Mura-Zala basin and accelerated subsidence in its hanging wall in Karpatian–Badenian time (17.3–13 Ma) may have completed this process.

Strike-slip faults with NE–SW to E–W compression marks the end of major extensional deformation in the area, which is frequently attributed to change in subduction geometry in the Carpathians (Peresson & Decker 1997; Fodor et al. 1999). The final stage of deformation, strike-slip faulting with N–S to NNW–SSE compression is part of a widespread transpressional deformation of the Dinaridic–Alpine–Pannonian junction.

#### Acknowledgements

Fieldwork campaigns were supported by two bilateral intergovernmental projects between Slovenia and Hungary (Slo5/98, Slo/6 00), donated to B. Jelen, N. Zupančič and L. Fodor (project leaders) and also by research programs in the Geological Institute of Hungary. K–Ar measurements were supported by National Scientific Found of Hungary (OTKA, project T043344, and M041434) donated to K. Balogh and Z. Pécskay, and the mineral chemical and thermobarometric studies by the grant No. F-047322/2004–2007 to P. Horváth. L. Fodor benefited from the Bolyai János scholarship of the Hungarian Academy of Sciences in 2000–2001 and 2006–2007. John Corckery contributed to the fieldwork. The paper benefited from the critical, but highly constructive reviews of C. Rosenberg, U. Schaltegger and S. Schmid. The authors are thankful for the careful and precise work of the staff at the RISØ and Oregon nuclear reactors. Deutsche Forschungsgemeinschaft (DFG) financed fission track analyses in the frame of the Collaborative Research Centre #275 in Tübingen. The authors are grateful for the careful sample preparation made by Dagmar Kost, Gerlinde Höckh and Dorothea Mühlbayer-Renner (Tübingen).

#### REFERENCES

Altherr, R., Lugović, B., Meyer, H.P. & Majer, V. 1995: Early Miocene post-collisional calc-alkaline magmatism along the easternmost segment of the Periadriatic fault system (Slovenia and Croatia). *Mineralogy and Petrology* 54, 225–247.

Angelier, J. 1984: Tectonic analysis of fault slip data sets. *Journal of Geophysical Research* 89, B7, 5835–5848.

Balen, D., Horváth, P., Tomljenović, B., Finger, F., Humer, B., Pamić, J. & Árkai, P. 2006: A record of pre-Variscan Barrovian regional metamorphism in the eastern part of the Slavonian Mountains (NE Croatia). *Mineralogy and Petrology* 87, 143–162.

Balogh, K. 1985: K–Ar dating of Neogene volcanic activity in Hungary: Experimental technique, experiences and methods of chronologic studies. Manuscript, internal report of the Nuclear Research Institute of Hungarian Academy of Sciences (ATOMKI), D/1, 277–288.

Balogh, K., Árva-Soós, E. & Buda, Gy. 1983: Chronology of granitoid and metamorphic rocks in Transdanubia (Hungary). *Annuaire de l'Institut de Géologie et Géophysique* 61, 359–364.

Benedek, K. 2002: Paleogene igneous activity along the easternmost segment of the Periadriatic-Balaton Lineament. *Acta Geologica Hungarica* 45, 359–371.

Benedek, K. & Zupančič, N. 2002: Periadriatic Intrusive Chain – version 1. In: Dunkl, I., Balintoni, I., Frisch, W., Hoxha, L., Janák, M., Koroknai, B., Milovanović, D., Pamić, J., Székely, B. & Vrabec, M. (Eds.): *Metamorphic Map and Database of Carpatho-Balkan-Dinaride Area*. <http://www.met-map.uni-goettingen.de>

von Blanckenburg, F. & Davies, J.H. 1995: Slab breakoff: A model for syn-collisional magmatism and tectonics in the Alps. *Tectonics* 14, 120–131.

Blundy, J.D. & Holland, T.J.B. 1990: Calcic amphibole equilibria and a new amphibole-plagioclase geothermometer. *Contributions to Mineralogy and Petrology* 104, 208–224.

Deleon, G. 1969: Overview on the results of the radiometric dating of the granitoid rocks in Yugoslavia (in Serbian). *Radovi Instituta Geološko-Rudarska Istraživanja Ispitivanja Nuklearnih Drugih Mineralnih Sirovina* 6, 165–182.

Dolar-Mantuani, L. 1935: Das Verhältnis der Aplite zu den Tonaliten im Massiv des Pohorje (Bäckergebirges). *Geoloski Anali Balkanskog Poluostrva* 12, 2, 1–165.

Dolenc, T. 1994: New isotopic and radiometric data related to igneous rocks of the Pohorje Mountains. *Rudarsko-metalurški zbornik* 41, 147–152.

Dunkl, I., Di Giulio, A. & Kuhlemann, J. 2001: Combination of single-grain fission-track chronology and morphological analysis of detrital zircon crystals in provenance studies – sources of the Macigno formation (Apennines, Italy). *Journal of Sedimentary Research* 71, 516–525.

Dunkl, I., Frisch, W. & Grundmann, G. 2003: Zircon fission track thermochronology of the southeastern part of the Tauern Window and the adjacent Austroalpine margin, Eastern Alps. *Eclogae Geologicae Helveticae* 96, 209–217.

Ebner, F. & Sachsenhofer, R. 1991: Die Entwicklungsgeschichte des Steirischen Tertiärbeckens. *Mitteilungen der Abteilung für Geologie und Paläontologie am Landesmuseum Joanneum Graz* 49, 96 pp.

Elias, J. 1998: The thermal history of the Ötztal-Stubai complex (Tyrol, Austria/Italy) in the light of the lateral extrusion model. *Tübinger Geowissenschaftliche Arbeiten, Reihe A*, 36, 172 pp.

Exner, C. 1976: Die geologische Position der Magmatite des periadriatischen Lineaments. *Verhandlungen der Geologischen Bundesanstalt* 3–64.

Faninger, E. 1970: Pohorski tonalit in njegovi diferencijati. *Geologija* 13, 35–104.

Fodor, L., Jelen, B., Márton, E., Skaberne, D., Čar, J. & Vrabec, M. 1998: Miocene–Pliocene tectonic evolution of the Slovenian Periadriatic Line and surrounding area – implication for Alpine-Carpathian extrusion models. *Tectonics* 17, 690–709.

Fodor, L., Csontos, L., Bada, G., Györfi, I. & Benkovic, L. 1999: Tertiary tectonic evolution of the Pannonian basin system and neighbouring orogens: a new synthesis of paleostress data. In: Durand, B., Jolivet, L., Horváth, F. & Séranne, M. (Eds.): *The Mediterranean Basins: Tertiary extension within the Alpine Orogen*. Geological Society, London, Special Publications, 156, 295–334.

Fodor, L., Jelen, B., Márton, E., Rifelj, H., Kraljić, M., Kevrić, R., Márton, P., Koroknai, B. & Báldi-Beke, M. 2002a: Miocene to Quaternary deformation, stratigraphy and paleogeography in Northeastern Slovenia and Southwestern Hungary. *Geologija* 45, 103–114.

Fodor, L., Jelen, B., Márton, E., Zupančič, N., Trajanova, M., Rifelj, H., Pécskay, Z., Balogh, K., Koroknai, B., Dunkl, I., Horváth, P., Horvat, A., Vrabec, M., Kraljić, M. & Kevrić, R. 2002b: Connection of Neogene basin formation, magmatism and cooling of metamorphic rocks in NE Slovenia. *Geologica Carpathica* 53, special issue, 199–201.

Frank, W. 1987: Evolution of the Austroalpine elements in the Cretaceous. In: Flügel, H.W. & Faupl, P. (Eds.): *Geodynamics of the Eastern Alps*. Deuticke, Vienna, 379–406.

Frisch, W., Kuhlemann, J., Dunkl, I. & Brügel, A. 1998: Palinspastic reconstruction and topographic evolution of the Eastern Alps during late Tertiary extrusion. *Tectonophysics* 297, 1–15.

- Frisch, W., Dunkl, I. & Kuhleemann, J. 2000: Postcollisional orogen-parallel large-scale extension in the Eastern Alps. *Tectonophysics* 327, 239–265.
- Galbraith, R.F. & Laslett, G.M. 1993: Statistical models for mixed fission track ages. *Nuclear Tracks and Radiation Measurements* 21, 459–470.
- Gerdes, A. & Zeh, A. 2006: Combined U-Pb and Hf isotope LA-(MC)-ICP-MS analyses of detrital zircons: Comparison with SHRIMP and new constraints for the provenance and age of an Armorican metasediment in Central Germany. *Earth and Planetary Science Letters* 249, 47–61.
- Gerdes, A. & Zeh, A. 2008: Zircon formation versus zircon alteration – new insights from combined U-Pb and Lu-Hf in situ LA-ICP-MS analyses, and consequences for the interpretation of Archean zircon from the Central Zone of the Limpopo Belt. *Chemical Geology*, doi 10.1016/j.chemgeo.2008.03.005.
- Green, P.F. 1981: A new look at statistics in fission track dating. *Nuclear Tracks* 5, 77–86.
- Hammarstrom, J.M. & Zen, E. 1986: Aluminium in hornblende: an empirical igneous geobarometer. *American Mineralogist* 71, 1297–1313.
- Hámor, G. 1985: Geology of the Nógrád-Cserhát area. *Geologica Hungarica series Geologica* 22, 234 pp.
- Hámor, G., Baranyai-Ravasz, L., Halmaj, J., Balogh K. & Árva-Soós, E. 1987: Dating of Miocene acid and intermediate volcanic activity in Hungary. *Annals of the Hungarian Geological Institute* 70, 149–154.
- Harangi, Sz., Mason, P.R.D. & Lukács, R. 2005: Correlation and petrogenesis of silicic pyroclastic rocks in the northern Pannonian Basin, Eastern central Europe: in situ trace element data of glass shards and mineral chemical constraints. *Journal of Volcanology and Geothermal Research* 143, 237–257.
- Hinterlechner-Ravnik, A. 1971: The Pohorje Mountains metamorphic rocks I. *Geologija* 14, 187–226.
- Hinterlechner-Ravnik, A. 1973: The metamorphic rocks of the Pohorje Mountains II. *Geologija* 16, 245–269.
- Hollister, L.S., Grissom, G.C., Peters, E.K., Stowell, H.H. & Sisson, V.B. 1987: Confirmation of the empirical correlation of Al in hornblende with pressure of solidification of calc-alkaline plutons. *American Mineralogist* 72, 231–239.
- Janák, M., Vrabec, M., Froitzheim, N. & de Hoog, C.-J. 2007: Kyanite eclogites and garnet peridotites from the Pohorje Slovenia: petrological constraints on the Cretaceous subduction and exhumation in the HP/UHP terrane of the Eastern Alps. Abstract volume of the 8<sup>th</sup> Workshop on Alpine Geological Studies, Davos, Switzerland, 10.–12. October 2007, 29–30.
- Jelen, B. & Rifelj, H. 2003: The Karpatian in Slovenia. In: Brzobohatý, R., Čiča, M., Kováč, M. & Rögl, F. (Eds.): *The Karpatian: A Lower Miocene Stage of the Central Paratethys*. Masaryk University, Brno, 133–139.
- Kieslinger, A. 1935: *Geologie und Petrologie des Bacher*. Verhandlungen der Geologischen Bundesanstalt 7, 101–110.
- Kőrösy, L. 1988: Hydrocarbon geology of the Zala Basin in Hungary. *Általános Földtani Szemle* 23, 3–162.
- Laubscher, H. 1983: The late Alpine (Periadriatic) intrusions and the Insubric Line. *Memorie della Societa Geologica Italiana* 26, 21–30.
- Leake, B.E., Woolley, A.R., Arps, C.E.S., Birch, W.D., Gilbert, M.C., Grice, J.D., Hawthorne, F.C., Kato, A., Kisch, H.J., Krivovichev, V.G., Linthout, K., Laird, J., Mandarino, J., Maresch, W.V., Nickel, E.H., Rock, N.S.M., Schumacher, J.C., Smith, D.C., Stephenson, N.C.N., Ungaretti, L., Whittaker, E.J.W., Youzhi, G. (1997) Nomenclature of amphiboles: Report of the Subcommittee on Amphiboles of the International Mineralogical Association Commission on New Minerals and Mineral names. *Mineralogical Magazine* 61, 295–321.
- Márton, E., Fodor, L., Jelen, B., Márton, P., Rifelj, H. & Kevrić, R. 2002: Miocene to Quaternary deformation in NE Slovenia: complex paleomagnetic and structural study. *Journal of Geodynamics* 34, 627–651.
- Márton, E., Trajanova, M., Zupančič, N. & Jelen, B. 2006: Formation, uplift and tectonic integration of a Periadriatic intrusive complex (Pohorje, Slovenia) as reflected in magnetic parameters and paleomagnetic directions. *Geophysical Journal International* 167, 1148–1159.
- Miller, C., Mundil, R., Thöni, M. & Konzett, J. 2005: Refining the timing of eclogite metamorphism: a geochemical, petrological, Sm-Nd and U-Pb case study from the Pohorje Mountains, Slovenia (Eastern Alps). *Contributions to Mineralogy and Petrology* 150, 70–84.
- Mioč, P. 1978: Geology of the sheet Slovenj Gradec L 33–55 1:100000. Federal Geological Survey of Yugoslavia, Belgrade, 74 pp.
- Mioč, P. & Žnidarčič, M. 1977: Geological map of the sheet Slovenj Gradec, L 33–55, 1:100000. Federal Geological Survey of Yugoslavia, Belgrade.
- Odin, G.S. et al. 1982: Interlaboratory standards for dating purposes. In: Odin, G.S. (Ed.): *Numerical Dating in Stratigraphy*. Wiley & Sons, Chichester, New York, Brisbane, 123–149.
- Pálffy J., Mundil R., Renne P.R., Bernor R.L., Kordos, L. & Gasparik, M. 2007: U-Pb and Ar-40/Ar-39 dating of the Miocene fossil track site at Ipolytarnoc (Hungary) and its implications. *Earth and Planetary Science Letters* 258, 160–174.
- Pálínkaš, L., & Pamić, J. 2001: Geochemical evolution of Oligocene and Miocene magmatism across the Easternmost Periadriatic Lineament. *Acta Vulcanologica* 13, 41–56.
- Pamić, J. & Pálínkaš, L. 2000: Petrology and geochemistry of Paleogene tonalites from the easternmost parts of the Periadriatic Zone. *Mineralogy and Petrology* 70, 121–141.
- Pécskay, Z. et al. 2006: Geochronology of Neogene magmatism in the Carpathian arc and intra-Carpathian area. *Geologica Carpathica* 57, 511–530.
- Peresson, H. & Decker, K. 1997: Far-field effect of late Miocene subduction in the eastern Carpathians: E-W compression and inversion of structures in the Alpine-Carpathian-Pannonian region. *Tectonics* 16, 38–56.
- Pischinger, G., Kurz, W. Übleis, M., Egger, M., Fritz, H., Brosch F.J. & Stingl, K. 2008: Fault slip analysis in the Koralm Massif (Eastern Alps) and consequences for the final uplift of “cold spots” in Miocene times. *Swiss Journal of Earth Sciences*, this volume.
- Ratschbacher, L., Frisch, W., Linzer, H.G. & Merle, O. 1991: Lateral extrusion in the Eastern Alps, part 2: structural analysis. *Tectonics* 10, 257–271.
- Rosenberg C. L. 2004: Shear zones and magma ascent: a model based on a review of the Tertiary magmatism in the Alps. *Tectonics* 23, TC3002, doi:10.1029/2003TC001526.
- Sachsenhofer, R. F., Dunkl, I., Hasenhüttl, Ch. & Jelen, B. 1998: Miocene thermal history of the southwestern margin of the Styrian Basin: coalification and fission track data from the Pohorje/Kozjak area (Slovenia). *Tectonophysics* 297, 17–29.
- Sachsenhofer, R.F., Jelen, B., Hasenhüttl, Ch., Dunkl, I. & Rainer, T. 2001: Thermal history of Tertiary basins in Slovenia (Alpine-Dinaride-Pannonian junction). *Tectonophysics* 334, 77–99.
- Salomon, W. 1897: Über des Alter, Lagerungsform, und Entstehungsart der Periadriatischen granitischkörnigen Massen. *Tschermaks Mineralogische und petrographische Mitteilungen Neue Folge* 17, 109–283.
- Schaltegger, U. & Corfu, F. 1992: The age and source of Late Hercynian magmatism in the Central Alps – evidence from precise U-Pb ages and initial Hf isotopes. *Contributions to Mineralogy and Petrology*, 111, 329–344.
- Scharbert, S. 1975: Radiometrische Altersdaten von Intrusivgesteinen im Raum Eisenkappel (Karawanken, Kärnten). *Verhandlungen der Geologischen Bundesanstalt* 4, 301–304.
- Schmid, S.M., Aebli, H.R., Heiler, F. & Zingg, A. 1989: The role of the Periadriatic line in the tectonic evolution of the Alps. In: Coward, M.P., Dietrich, D. & Park, R.G. (Eds.): *Alpine tectonics*. Geological Society, London, Special Publications 45, 153–171.
- Schmid, S.M., Fügenschuh, B., Kissling, E. & Schuster, R. 2004: Tectonic map and overall architecture of the Alpine orogen. *Eclogae Geologicae Helvetica* 97, 93–117.
- Schmidt, M.W. 1992: Amphibole composition in tonalite as a function of pressure: an experimental calibration of the Al-in-hornblende barometer. *Contributions to Mineralogy and Petrology* 110, 304–310.
- Slama, J., Košler, J., Condon, D.J., Crowley, J.L., Gerdes, A., Hanchar, J.M., Horstwood, M.S.A., Morris, G.A., Nasdala, L., Norberg, N., Schaltegger, U., Schoene, B., Tubrett, M.N. & Whitehouse, M.J. 2008: Plešovice zircon – a new natural reference material for U-Pb and Hf isotopic microanalysis. *Chemical Geology* 249, 1–35.
- Sölva, H., Stüwe, K. & Strauss, P. 2005: The Drava River and the Pohorje Mountain Range (Slovenia): geomorphological interactions. *Mitteilungen des Naturwissenschaftlichen Vereines für Steiermark* 134, 45–55.
- Steenken, A., Siegesmund, S., Heinrichs, T. Fügenschuh, B. 2002: Cooling and exhumation of the Rieserferner Pluton (Eastern Alps, Italy/Austria). *International Journal of Earth Sciences* 91, 799–817.

- Steiger, R.H. & Jäger, E. 1977: Subcommittee on geochronology – convention on use of decay constants in geochronology and cosmochronology. *Earth and Planetary Science Letters* 36, 359–362.
- Steininger, F., Müller, C. & Rögl, F. 1988: Correlation of Central Paratethys, Eastern Paratethys, and Mediterranean Neogene stages. In: Royden, L.H. & Horváth, F. (Eds.): *The Pannonian Basin*. American Association of Petroleum Geologists Memoir 45, 79–87.
- Tari, G., Horváth, F. & Rumpler, J. 1992: Styles of extension in the Pannonian Basin. *Tectonophysics* 208, 203–219.
- Thöni, M. 2002: Sm–Nd isotope systematics in garnet from different lithologies (Eastern Alps): Age results and an evaluation of potential problems for garnet Sm–Nd chronometry. *Chemical Geology* 185, 255–281.
- Trajanova, M. 2002: Significance of mylonites and phyllonites in the Pohorje and Kobansko area. *Geologija* 45, 149–161.
- Trajanova, M., Pécskay, Z. & Itaya, T. 2008: K–Ar geochronology and petrography of the Miocene Pohorje Mountains batholith (Slovenia). *Geologica Carpathica* 59, 247–260.
- Vrabec, M., Pavlovčič-Prešeren, P. & Stopar, B. 2006: GPS study (1996–2002) of active deformation along the Periadriatic fault system in northeastern Slovenia: tectonic model. *Geologica Carpathica* 57, 57–65.
- Wedepohl, K.H. 1995: The composition of the continental crust. *Geochimica et Cosmochimica Acta* 59, 1217–1232.
- Winkler, A. 1929: Über das Alter der Dacite Gebiet des Dradurchbruchs. *Verhandlungen der Geologischen Bundesanstalt* 169–181.
- Žnidarčič, M. & Mioč, P. 1988: Geological map of the sheets Maribor and Leibnitz, L 33–56 and L 33–44, 1:100 000. Federal Geological Survey of Yugoslavia, Belgrade.
- Zupančič, N. 1994a: Petrografske značilnosti in klasifikacija pohorskih magmatskih kamnin. *Rudarsko-metalurški zbornik* 41, 101–112.
- Zupančič, N. 1994b: Geokemične značilnosti in nastanek pohorskih magmatskih kamnin. *Rudarsko-metalurški zbornik* 41, 113–128.

Manuscript received 18 January, 2008

Revision accepted 8 July 2008

Editorial Handling: Stefan Schmidt & Stefan Bucher